



Project funded by the European Commission under the 6th (EC) RTD Framework Programme (2002- 2006) within the framework of the specific research and technological development programme "Integrating and strengthening the European Research Area"



## Project UpWind

Contract No.:  
019945 (SES6)

"Integrated Wind Turbine Design"



---

# Probabilistic Strength Assessment of Rotor Blades

---

|                  |   |
|------------------|---|
| AUTHOR:          | D. J. Lekou   |
| AFFILIATION:     | Centre for Renewable Energy Sources                             |
| ADDRESS:         | 19 <sup>th</sup> km Marathonos Ave., Pikermi, GR-190 09, Greece |
| TEL.:            | +30 210 6603300   |
| EMAIL:           | <a href="mailto:dlekou@cres.gr">dlekou@cres.gr</a>              |
| FURTHER AUTHORS: | T. P. Philippidis, K. C. Bacharoudis                            |
| REVIEWER:        |   |
| APPROVER:        |   |

### Document Information

|                 |   |
|-----------------|---|
| DOCUMENT TYPE   | Deliverable                                       |
| DOCUMENT NAME:  | Probabilistic Strength Assessment of Rotor Blades |
| REVISION:       | 0   |
| REV.DATE:       | 10.02.2011  |
| CLASSIFICATION: | R3: Restricted to WP3 members + PL                |
| STATUS:         | S3: Draft for comments                            |

**Abstract:** This document was prepared in the frame of Task 3.3 "Damage Tolerant Design Concept" of Work-Package WP3 "Rotor Structure and Materials" of the UPWIND project. Numerical procedures for determining the

strength of a rotor blade by taking into account the stochastic nature of anisotropic material properties as well as the stochastic loading imposed on the blade are in detail described. Based on earlier developed procedures within the frame of the UPWIND project, methodologies were built up for quantifying the blade design reliability. Specifically, the Edgeworth Expansion Technique and the Response Surface Method are applied for the reliability estimation of composite material blades. Results are compared with simulation predictions of the Monte Carlo method and are found in good agreement. The methodology based on the Edgeworth Expansion Technique results in non-conservative output, if the variability of the basic variables is quite high. However, the methodology developed has a number of advantages compared to the Monte Carlo simulation, since the procedure does not involve iterative solutions for the reliability estimation. This is an important feature during the design phase where a lot of solutions need to be checked. The Response Surface Method is more accurate, yet again iterative. Both developed procedures enable direct connection with state of the art aeroelastic simulation tools used for wind turbines. This makes the methods attractive for application during the design of wind turbine rotor blades, where a probabilistic approach of the problem is expected to offer new potential in the direction of optimized material use.

# Contents

|       |  |    |
|-------|--|----|
| 1.    | Introduction .....   | 4  |
| 2.    | Structural analysis.....   | 5  |
| 2.1   | Finite Element Models .....  | 5  |
| 2.2   | PRE-, POST-THIN (Sectional analysis).....  | 6  |
| 3.    | Input variables.....   | 8  |
| 3.1   | Material Properties .....  | 8  |
| 3.2   | Loads.....   | 9  |
| 3.2.1 | Loading and Finite Element Blade Models.....   | 12 |
| 4.    | Probability of failure .....   | 14 |
| 4.1   | Lamina failure probability.....  | 14 |
| 4.2   | Laminate failure probability.....  | 14 |
| 4.3   | Failure probability of the blade section .....   | 16 |
| 5.    | Probabilistic methods.....   | 16 |
| 5.1   | Response Surface Method (RSM).....   | 17 |
| 5.2   | Edgeworth Expansion Method (EDW).....  | 18 |
| 5.3   | Monte Carlo method .....   | 19 |
| 6.    | Examples and discussion .....  | 20 |
| 6.1   | Effect of variability in strength, elasticity and loads in blade reliability (EDW, MC) ..... | 20 |
| 6.1.1 | Introducing loading variability .....  | 25 |
| 6.2   | RSM and Finite Element Model Application .....   | 28 |
| 6.2.1 | Reliability analysis .....   | 28 |
| 6.2.2 | Validation of the result .....   | 30 |
| 6.3   | RSM and EDW assessment using THIN .....  | 32 |
| 7.    | Conclusions .....  | 34 |
| 8.    | References.....  | 35 |

| STATUS, CONFIDENTIALITY AND ACCESSIBILITY |                    |                 |           |                                    |               |                  |
|---|--------------------|-----------------|-----------|------------------------------------|---------------|------------------|
| Status                                    |                    | Confidentiality |           |                                    | Accessibility |                  |
| <b>S0</b>                                 | Approved/Released  |                 | <b>R0</b> | General public                     |               | Private web site |
| <b>S1</b>                                 | Reviewed           |                 | <b>R1</b> | Restricted to project members      |               | Public web site  |
| <b>S2</b>                                 | Pending for review |                 | <b>R2</b> | Restricted to European. Commission |               | Paper copy       |
| <b>S3</b>                                 | Draft for comments | <b>X</b>        | <b>R3</b> | Restricted to WP members + PL      | <b>X</b>      |                  |
| <b>S4</b>                                 | Under preparation  |                 | <b>R4</b> | Restricted to Task members +WPL+PL |               |                  |

PL: Project leader    WPL: Work package leader    TL: Task leader

## 1. Introduction

The application of probability methods in the field of wind turbines and especially for the wind turbine blades is relative new. The need for probabilistic models for both loads and mechanical material properties became more evident during the last years, in an effort to reduce the cost of the structures. The issue has been addressed in earlier work regarding the failure of the blade root section due to bending moments developed against fatigue e.g. [1], [2], as well as against ultimate loading, e.g. [3]. In [3] the first order reliability method (see e.g. [4], [5]) was applied for the estimation of the reliability in all cases, through the implementation of commercially available code PROBAN [6], while the commercial available code STRUREL [7] has been implemented in FAROW [8], a more general tool for fatigue calculations and reliability estimations of wind turbine components, focusing in modelling the interaction between the environment, the load response to the environment and the cumulative damage process underlying the lifetime calculation. The applications presented, e.g. [1], [2] and [3] were limited to estimating the reliability of the root section of the blade, which is usually symmetrically built, taking into account only the developed stress in the axial direction due to bending in the flap direction and the respective strength of the laminate. Yet, the root section is not always the critical section of a blade, which is designed for optimized material use throughout the blade length.

The sections along the blade length are usually thin to thick walled multi-cellular, non-symmetrical, heterogeneous constructions of multilayered composite laminates. To accurately predict failure (or non-failure) of the blade, a point to point assessment of the strength on any location of the blade is necessary, using analysis applicable to multilayered composite components, taking into account not only the developed axial normal stresses, i.e. along the blade length, but the complex in-plane stress field in the principal coordinate system of each ply along with the associated anisotropy in strength.

To this end, probability techniques for reliability analysis of composite materials are suitable. As will be discussed in the following sections of the present document, the use of composite materials in the blade structure and the many stochastic variables that are thus involved in the analysis along with the higher complexity of the existing probabilistic methods makes the available reliability estimation methods and software codes not attractive for integration in the design procedure, where a large number of loading cases has to be checked against a number of alternatives in terms of structural properties.

To improve this, in this work, performed within the frame of the UPWIND project under Work Package 3 [9], numerical tools were especially developed for the probabilistic strength analysis of rotor blades made of composite materials. Two different structural models of the blade were employed, namely a full 3D Finite Element shell model of commercial code ANSYS, as well as a sectional model of the blade. Regarding probabilistic methods, two techniques were assessed through various examples and compared with Monte Carlo (MC) simulation results, specifically the Response Surface Method (RSM) and the Edgeworth Expansion Technique (EDW).

Common to the developed methodologies is that the probability estimations are conducted by performing a ply-by-ply analysis using the quadratic version of the failure tensor polynomial, Tsai-Hahn [10], taking into account the heterogeneous built up of the blade. Also, the reliability estimation tools developed for the probabilistic strength assessment of rotor blades and presented herein consider the stochastic nature of the anisotropic material properties (both in terms of elasticity and strength) as well as the loads for the reliability estimation of the layer and thereupon extended to the laminate, the blade section and the overall blade.

These methodologies will be presented in the following sections and their advantages and disadvantages regarding application during the design of the blade will be thoroughly discussed.

## 2. Structural analysis

Wind turbine blades are composite material structures designed for safe life, contrary to the alternative method of designing a structure for failing safe. The operational life of the blades, so as to enable sustainable application of wind energy systems regarding cost is 20 years, while recent studies for offshore applications come to set new limits for the operational life at 30 years. The loading imposed on blades during their operational life is synthesized from various stochastic and deterministic cases that are determined by large load variations due to the irregularity of wind speed and direction, turbulence intensity and the effects of site terrain.

Contemporary wind turbine blades have cross-sections that are usually thin to thick walled multi-cellular constructions of multilayered composite laminates. A typical cross-section of the blade is shown in Figure 1, where the location of unidirectional layers (UD) in the spar caps to carry the axial loading developed, the foam to prevent from local buckling and the general lamination sequences, comprising bi-directional layers, to undertake the shear loading developed on the section is shown.

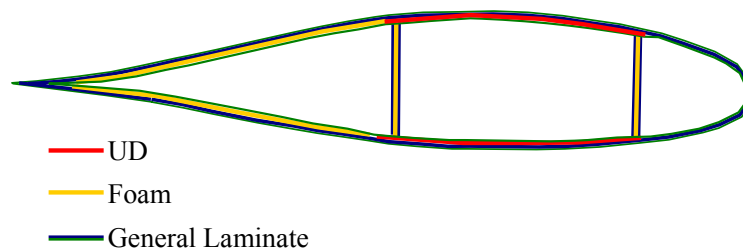


**Figure 1 Typical cross-section of blade**

For the design of wind turbine blades, the international standard IEC-61400-1 [11] is followed. This standard was developed to alleviate differences between national standards and guidelines that were extensively used during the initial phases of wind energy development, such as GL [12] and DNV [13].

### 2.1 Finite Element Models

To perform a detailed structural design of the blade examining the internal stress distribution within the blade a 3-D finite element model of the blade is necessary [14], comprising thousands of composite shell elements, typically using large commercial finite element analysis codes (e.g. [15], [16]). The finite element model of the blade used as an example for the application of the developed probabilistic methodologies has the above mentioned characteristics.

The case study was performed for a 30m Glass/Polyester blade developed in the frame of the EC funded MEGAWIND project [17]. Initially the blade manufactured and tested was modular with an intermediate joint at 12.4m, while it was designed according to the applicable at the time edition 2 of IEC 61400-1 [18]. For the purposes of the present work, the blade was redesigned, keeping more or less the same mass and stiffness distributions. Bolted connections and all the metallic parts of the intermediate joint were removed, together with the relevant unnecessary layers at the joint area. The blade model is loaded by the design value loads for ultimate strength analysis as described in Annex F of the 3<sup>rd</sup> edition of the international standard [11]. The finite element (FE) model of the blade created using commercial code ANSYS, see Figure

1, consists of more than 2,000 SHELL181 4-node elements. The layered, anisotropic shell is based on the Reissner-Mindlin shear deformation theory through the thickness. All nodal degrees of freedom at the blade root were constrained to simulate blade attachment to the hub, while concentrated forces were applied to reproduce the loading distribution as derived from design load definition, as discussed in a following section of the present document. More details on the model can be found in [19].

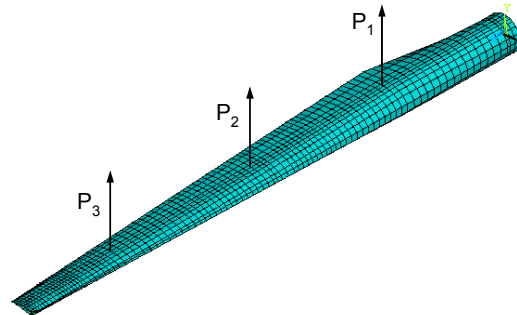


**Figure 2: FE model of 30m GI/P blade**

However, this type of finite element models although necessary for the final blade designs are too costly [14] and too detailed [20] for direct use in a system of aeroelastic analysis. At the same time, the size of Multi-MW-sized blades require blade designers to consider the structure of the blade earlier in the design process [14], thus a closer, effective interaction between codes performing aero-elastic analysis for the wind turbine system and tools used for the blade structural design is crucial. Current state of the art aero-elastic tools, used for the prediction of loading on the rotor blades but also for the assessment of the whole wind turbine, model the blades encompassing finite elements with beam formulation, specially adapted for more accurate predictions of the wind turbine response (e.g. [21], [22]).

## 2.2 PRE-, POST-THIN (Sectional analysis)

In order to take advantage of the available aero-elastic codes, but also accurately represent the mechanical properties of the full 3-dimensional blade in the 1-dimensional beam element, for the load estimation using aero-elastic codes, and be able to perform the necessary detailed strength assessment after stress resultants at each section have been calculated, the developed tool has been divided into 3 modules: PRE-THIN, THIN and POST-THIN. A short description of each of these modules is given in the following, considering a typical cross-section of a blade as shown in Figure 1. A schematic presentation of each module input and output data (presented as parallelograms) as well as their interaction is shown in Figure 3, where each module is presented as a rectangle. More details for the developed tool were presented in [23]. It should be noted that in the current work the aero-elastic code is considered as an independent tool and its output is a necessary input of THIN module.

PRE-THIN is the module where using the detailed input for the material properties, as well as the information on the lamination sequences used at each location on the section, the effective properties of each laminate are calculated using Classical Lamination Theory (CLT) approach. Specifically, the material properties needed as input are the mass density and the elastic properties of each orthotropic layer used in any lamination sequence in the section, namely the elasticity modulus in the two main directions of the orthotropic medium, the in-plane Poisson ratio and the in-plane shear modulus of the layer. These are used to estimate the homogenized multilayer construction effective properties, namely the total thickness of the laminate, the mass density and the elasticity and shear modulus on the primary laminate axis (considered to correspond with the blade axis).

For the probabilistic analysis both the strength properties and the 4 elastic layer properties of each material used in the section of each layer are assumed to be stochastic. For these variables, namely the strength and elasticity properties of the different materials, appropriate statistical information are necessary as input in the PRE-THIN module.

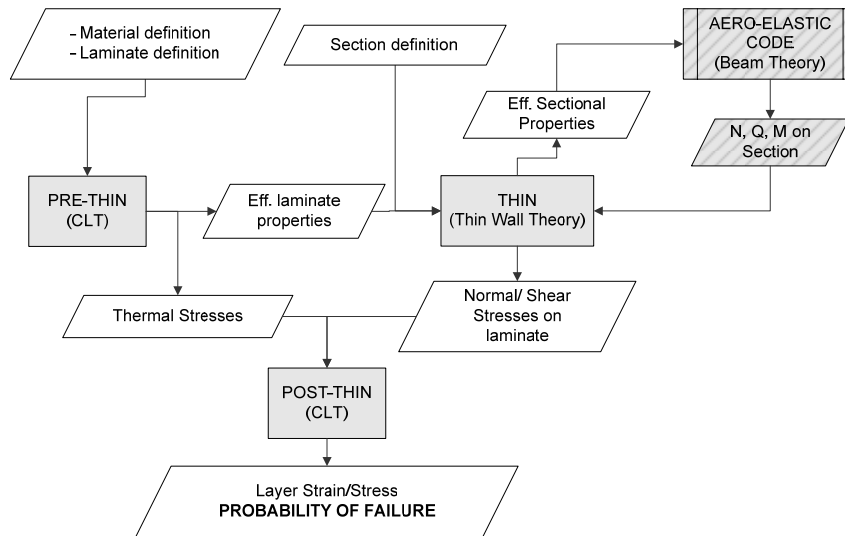


**Figure 3 Schematic flow-diagram of the developed tool (patterned boxes imply independent tools/data)**

The effective properties calculated for each laminate, together with their statistical properties in a reliability assessment, are fed as input into the main calculation module, THIN. For the detailed layer-by-layer strength analysis all material and lamination information, including the calculated stiffness matrix, comprising the extensional, A, coupling, B, and bending, D, stiffness matrix, as well as its inverse of each laminate are fed into the post processing module, POST-THIN.

At this point it should be mentioned that although there are available tools for extracting the three-dimensional information of composite rotor blades into one-dimensional beam elements, e.g. [24], [25], there are less work dealing with transforming the one-dimensional results of aero-elastic codes to detailed internal strain/stress analysis of the three-dimensional structure. This is, nevertheless, an essential step in the loop during the structural design of the wind turbine blade, if detailed finite element analysis is to be kept to a minimum, while keeping up to date information on the necessary structural modifications of the blade during the complete aero-elastic analysis of the wind turbine.

The basic processor, THIN, which is based on thin wall beam theory, taking into account the inhomogeneity and elastic anisotropy of the cross-sectional elements, has been described in detail and validated in [26] for the deterministic case. The processor, estimates for each section of the blade the mass centre, the elastic centre, the shear centre and the sectional properties, with respect to the mass weighted centre, for the case of line mass,  $\rho A$ , mass inertia in the edge (lead-lag) and flap direction,  $\rho I_y$  and  $\rho I_z$ , respectively, cross-mass inertia,  $\rho I_{yz}$  and polar mass inertia,  $\rho I_p$ , or the modulus weighted centre of the section, for the case of axial stiffness, EA, bending stiffness in the edge and flap direction,  $EI_y$  and  $EI_z$ , respectively, cross-bending stiffness,  $EI_{yz}$ , and torsional stiffness, GJ, through the input of the effective laminate properties derived through PRE-THIN. These might then be used with available aero-elastic finite element tools to simulate the behaviour of the wind turbine and calculate stress resultants in each blade section.

The aero-elastic simulation codes provide (for each load case) the internal resultant axial and shear forces, N,  $Q_y$  and  $Q_z$ , respectively and the internal resultant bending and torsional

moments,  $M_z$ ,  $M_y$  and  $M_x$ , respectively, at each selected section. These are used as input by THIN, to perform the detailed analysis on the section. In other words, from the stress resultants of the entire cross-section, as derived by the aero-elastic code, implementing beam finite element formulation, the stress resultants in the walls of each element composing the in-homogenous section are estimated within THIN processor. Its output is fed to POST-THIN module to estimate the three in-plane stress components of each ply in the laminated walls of the in-homogenous section. In addition to the stress resultants due to mechanical load, the thermal stress resultants (axial and flexural) are also estimated and taken into account. That means, normal stress resultants for each "homogenized" element on the section are calculated due to the axial force, the bending moments and the hygro-thermal effects, constant shear flows due to torsion are calculated for each cell of the multi-cell thin-walled structure, as well as the shear flows due to the shear forces, as described in [26]. Thus, for each node on every element the normal and shear stress resultants are provided as output from the THIN processing module to POST-THIN module.

For the probabilistic analysis appropriate statistical information for the developed sectional internal force and moment resultants (axial and shear forces, flexural and torsional moment resultants) from the aero-elastic simulation codes are required as input to THIN.

POST-THIN is the post-processing module of the analysis, where using as input the material and lamination properties provided by PRE-THIN, as well as the average normal and shear stress at each element node on the section, the stress field and reliability of each layer in the lamination sequence is calculated.

### 3. Input variables

As already mentioned, the probabilistic applications described in this document assume as stochastic the material properties and the loads on the blade structure. All other model parameters, e.g. the layer thickness, the geometry of the blade, etc. are considered to be deterministic. In the present section only the requirements for stochastic input variables will be discussed.

#### 3.1 Material Properties

Following GL [12] and DNV-OS-J102 [13] the material properties to be used in the design of a blade should be determined (through experiments) at the layer level. Thus, for the methodologies developed in here these material properties at the layer level are considered as the necessary input parameters.

Composite materials exhibit great inherent variability of mechanical properties mainly due to their inhomogeneous nature and manufacturing methods. Previous studies, e.g. [27], [28], have underlined the importance of incorporating not only the variability of strength properties, but also the variability in the elastic material properties in probabilistic analysis of composite material structures.

For the statistical characterization of the variability of the material parameters experimental databases are used, covering information not only for the strength properties of the orthotropic media but also for the relevant elastic properties, such as [27], [29] and [30]. For the appropriate characterisation of the random variables, the experimental data are statistically analysed. This analysis includes estimation of descriptive statistics for the different samples, calculation of empirical distributions and parameter estimation of statistical model distributions (Weibull, Lognormal, Normal etc.) with appropriate methods such as the method of moments or the maximum likelihood. Hypothesis testing follows the analysis using various statistical tests such

as Kolmogorov-Smirnov and Anderson-Darling to assess the goodness of fit to the corresponding empirical distribution.

Depending on the theoretical background of the selected distributions, appropriate modifications might be required during the probabilistic estimation of the blade failure. For example, the assumption that an elastic material property (which is positively defined), such as the in-plane shear modulus,  $G_{12}$ , follows the normal distribution (for which the random variable is by definition in the  $(-\infty, +\infty)$  range) might require suppression of possible negative values during random number generation if the coefficient of variation of the property is relatively high.

The necessary statistical parameters to describe each property depend of course on the selected probabilistic method. For example, Monte Carlo simulation requires the definition of the statistical distribution and the parameters thereof, while the method based on Edgeworth Expansion requires the statistical moments of the parameter, i.e. mean value, variance, etc (see e.g. [19], [23]).

## 3.2 Loads

A major task in estimating rotor blade reliability is the stochastic modelling of the loading. Substantial research efforts were directed towards load uncertainty investigation by representing efficiently the stochastic wind conditions (wind speed, turbulence) and so for the extreme wind loads [31], [32], [33], [34], [35]. Research results were already incorporated in the last edition of IEC 61400-1 (3rd edition) [11].

As already implied, the loads to be used in the design of a wind turbine and therefore, a wind turbine blade, are the results of dynamic aero-elastic simulations. The loads are delivered in form of time series, covering all load cases and conditions prescribed in the IEC 61400-1 [11]. Modern available aero-elastic analysis tools (e.g. [21], [22]) deliver these time series for the wind turbine blades as sectional stress resultants, incorporating the effect of aerodynamic, gravitational and inertial loads acting on the blade.

Since ultimate strength analysis is investigated in the present study, the loads can be modelled by the distribution of the extreme maximum values within a given reference period as simple random variables, making the problem a time invariant reliability problem. In [19] the procedure described in Annex F of the IEC 61400-1 [11] for the estimation of the extreme distribution of the stress resultants using extrapolation on any blade section was followed and explicitly described. In here only the major steps will be presented and discussed.

The application was performed for the power production state of the wind turbine implementing the Normal Turbulence Model for various wind speed bins in the interval cut-in to cut-out wind speed,  $[v_{in}, v_{out}]$ . Local maxima of stress resultants from available 10-minute aeroelastic simulations are extracted with the peak over threshold method. The threshold value suggested by IEC 61400-1 [11] is equal to the mean value plus 1.4 times the standard deviation, although ongoing discussions suggested a careful selection of the threshold value [35]. Indeed, the choice of the threshold must solve a challenging problem. A low threshold value will generate too many points in the sample of the extremes, thus affecting the accurate modelling of the distribution of the extremes. On the other hand, a high threshold value would reduce the number of observations in the sample, thus creating the need to increase the number of aero-elastic simulations and therefore the cost of the procedure.

Several distributions, such as Gumbel, Normal, Lognormal, 2 and 3-parametric Weibull, were fitted to the local maxima samples in [19] using various statistical methods (Method of Moments, Maximum Likelihood Method, Least Squares Fit) followed by goodness of fit tests (Anderson-Darling, Kolmogorov-Smirnov), a procedure similar to the procedures applied for the statistical characterization of the material parameters. An example of the distribution fitting on a Gumbel plot is presented in Figure 4(a) for an inboard section of the blade and a specific wind speed bin

of 23m/s. Preferred fitting was obtained by the Gumbel distribution (black solid line), denoted as “new Gumbel” in the graph, obtained using least squares estimates on a limited part of the data with the purpose to best fit the maximum values [19]. The Gumbel distribution used has the form:

$$F(x) = \exp\left(-\exp\left(\frac{-(x-b)}{a}\right)\right) \quad \text{Eq. 1}$$

The procedure for the probability function of the local maxima is repeated for every wind speed bin (obtaining more than 10 Gumbel distributions, depending on the wind speed range of the bin and the wind speed range for the normal operation of the wind turbine). The distribution for the probability of exceedance of the extreme stress resultant is derived as the long term probability, in terms of the partial distributions for each wind speed bin, given by:

$$P(F_{ext} \geq F | T = 10 \text{ min}) = \int_{v_{in}}^{v_{out}} P(F_{ext} \geq F | V, T) p(V) dV \quad \text{Eq. 2}$$

Results of these exceedance probability distributions are shown for the same example in Figure 4(b), along with the probability of  $P_e(F_R) = 3.8E-7$ , used for determining the characteristic design load following IEC 61400-1 and the maximum stress resultant obtained in the simulation data for the specific section.

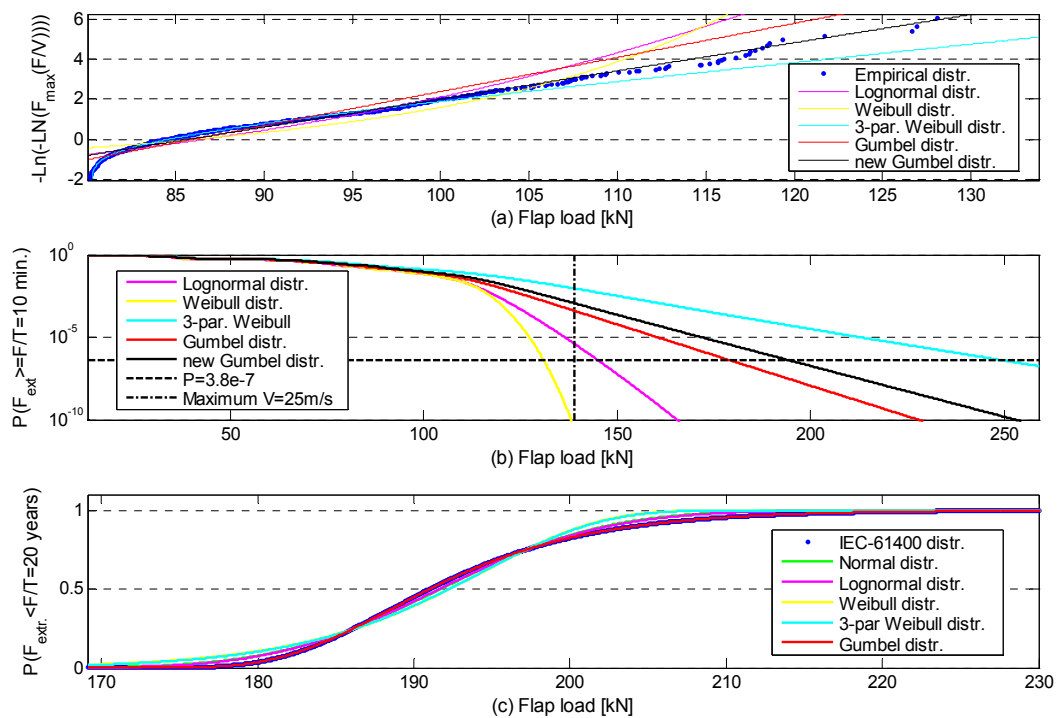


**Figure 4: Flap shear force at inboard section: (a) Gumbel plot (for mean wind speed  $V=23\text{m/s}$ ), (b) exceedance probability distribution (all wind speeds), (c) 20 year extreme distributions**

In [19] it was assumed for simplicity that the wind turbine operates for twenty years in power production state. It was further assumed that twenty years consist of  $N=1,051,200$  independent

10 minute intervals and thus the long term probability of the extreme concentrated load for twenty years period was given by [36]:

$$P(F_{ext} \leq F|T = 20\text{yr}) = (1 - P(F_{ext} > F|T = 10\text{min}))^N \quad \text{Eq. 3}$$

The term  $P(F_{ext} > F|T = 10\text{min})$  corresponds to the distributions of Figure 4(b) (and solution of Eq.2). As an example, the estimated long term extremes for the twenty years are presented in Figure 4(c) (blue dots).

The probability distribution functions of the corresponding load random variables to be used with the reliability calculations are based on fitting of the estimated long term extremes for the twenty years. Again, various typical distributions (Normal, Lognormal, Gumbel, 2 and 3-parametric Weibull) were fitted in [19] to the 20-year long term distributions, Eq. (3), using least squares. Results for the example case (for one section and one loading component) are also shown in Figure 4(c) (coloured lines). Also for this case, the Gumbel distribution fits satisfactorily the discrete points from the distribution of the extreme 20 year results.

While the material parameters are assumed to be uncorrelated, this assumption cannot be easily adopted for load components on the blade section. To investigate the correlation of among the 6 components of the stress resultants at each section of the blade a suitable analysis should be conducted. This was part of a study [37], where the available aeroelastic simulation time series results, i.e. three simulations per wind speed bin (with a total of 12 wind speed bins) were employed. The correlation matrix was estimated as the mean of the 36 values of correlation coefficients for each section and as an example from [37], the matrix of an inboard blade section is presented in Table 1.

**Table 1:** Correlation matrix for the stress resultants of an inboard blade section

|                               | <b>N<br/>(Axial)</b> | <b>M<sub>x</sub><br/>(Torque)</b> | <b>M<sub>z</sub><br/>(Flap)</b> | <b>Q<sub>y</sub><br/>(Flap)</b> | <b>M<sub>y</sub><br/>(Edge)</b> | <b>Q<sub>z</sub><br/>(Edge)</b> |
|-------------------------------|----------------------|-----------------------------------|---------------------------------|---------------------------------|---------------------------------|---------------------------------|
| <b>N (Axial)</b>              | 1.00                 | 0.01                              | 0.08                            | 0.02                            | 0.00                            | 0.00                            |
| <b>M<sub>x</sub> (Torque)</b> | 0.01                 | 1.00                              | 0.44                            | 0.4                             | 0.84                            | 0.85                            |
| <b>M<sub>z</sub> (Flap)</b>   | 0.08                 | 0.44                              | 1.00                            | 0.96                            | 0.27                            | 0.26                            |
| <b>Q<sub>y</sub> (Flap)</b>   | 0.02                 | 0.4                               | 0.96                            | 1.00                            | 0.14                            | 0.13                            |
| <b>M<sub>y</sub> (Edge)</b>   | 0.00                 | 0.84                              | 0.27                            | 0.14                            | 1.00                            | 0.99                            |
| <b>Q<sub>z</sub> (Edge)</b>   | 0.00                 | 0.85                              | 0.26                            | 0.13                            | 0.99                            | 1.00                            |

Obviously, for the presented case, the axial component is an uncorrelated variable while flap, edge and torsion are correlated at various degrees. Therefore, the light-shaded part of the correlation matrix should be taken into account in a reliability analysis.

The above described should be repeated for every section of the blade where aeroelastic simulation results are available. Then this information should be fed into structural analysis codes for the estimation of the reliability of the blade. In the case of codes, such as THIN [23], where a sectional analysis of the blade is performed this procedure is straight forward. However, if 3D shell models are used for the stress analysis, to increase accuracy, a method should be developed for the stochastic representation of concentrated loads acting on the FE model.

### 3.2.1 Loading and Finite Element Blade Models

Since the loading of the blade is available stress resultants on specific sections along the blade length obtained through aeroelastic simulations of the beam model, this has to be properly converted to be applied as external loading on the 3D finite element model of the blade. The definition of an equivalent system is therefore required, which can be performed by appropriately modifying the methodology used for the evaluation of the blade strength on the basis of load component distribution during blade testing (see [38]).

The procedure has been presented in [19] to convert the flap moment distribution, obtained from the aero-elastic beam model to an equivalent system of concentrated forces acting on the blade for the 3D shell finite element model for a probabilistic analysis. To do that, in [19] the time series simulation results for each section of the blade have been converted to time series of concentrated forces along the blade length to obtain the same bending moment distribution (for every simulation time step). Then, the procedure for obtaining the long term (statistical) distribution of extremes for each component presented previously, has been applied, this time for each of the concentrated forces along the blade length using the time series.

Similar to the thoughts for the correlation among the load components on a blade section a closer look at the correlation among the loads, this time along the length of the blade is considered necessary. Thus, following the determination of the statistical distributions for the concentrated loads along the blade length, an evaluation of the correlation between these forces should be performed. In [19] this has been performed using the calculated time series of the concentrated loads and correlation coefficients has been estimated for each of the available twelve wind speed bin results encompassing three simulation results, i.e. 36 load cases in total. Assuming that only three concentrated forces will be applied along the blade length on the 3D finite element model, an example of the findings is presented in Figure 5. In this figure the correlation coefficients ( $r_{12}$ ,  $r_{13}$ ,  $r_{23}$ ) between concentrated forces at positions  $L_1$ ,  $L_2$  and  $L_3$  from the blade root ( $L_3$  being outboard) are shown obtained for each available simulation time series. The abscissa value of 1 corresponds to the first simulation of the first wind speed bin ( $v_{in}$ ) and so forth up to value 36 corresponding to the third simulation of the last wind speed bin ( $v_{out}$ ).

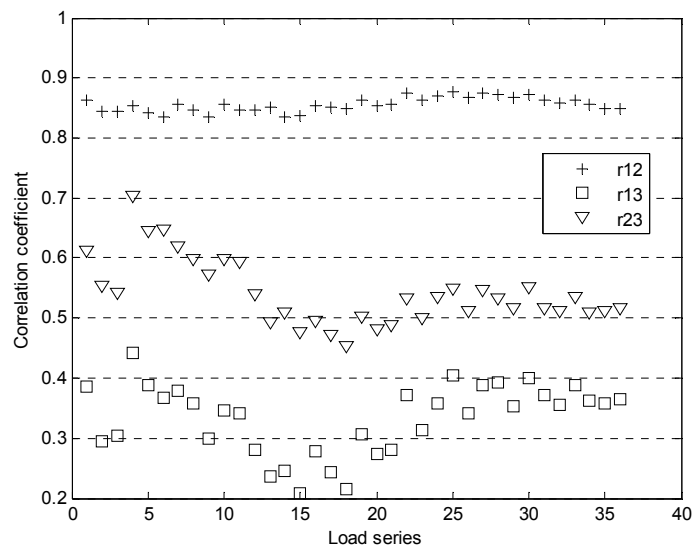


**Figure 5: Correlation coefficients estimation among the three concentrated forces along the blade length ( $r_{12}$ ,  $r_{13}$ ,  $r_{23}$ ) through time series**

From Figure 5 the correlation between the loads at positions  $L_1$  and  $L_2$  of the blade is very high for all simulations independently of mean wind speed. The loads at  $L_2$  and  $L_3$  are also highly

correlated this time with greater variation from one simulation to another even in the same wind speed bin. Finally, same trend with the latter holds for the correlation between loads at  $L_1$  and  $L_3$  which, as expected, have much lower correlation coefficient values. Therefore, it is readily concluded from Figure 5 that correlations among the three loads do exist and should be taken into account in a probabilistic analysis. In [19] this was performed using the mean value of the 36 results for the correlation coefficient.

Finally, although the question of the accuracy of the determination of an equivalent external loading system of forces applicable to the 3D shell finite element model of a blade, to replace the sectional stress resultants obtained through aeroelastic simulations, falls out of the scope of the present study, it is considered relevant to reproduce in here the findings of [19] on the subject.

The flap moment distribution, as defined through the stress resultant time series, i.e. the flap moment distribution induced by the external loads, must be close to the corresponding flap moment distribution resulting from the concentrated load time series. A direct comparison of these two distributions, that is as obtained from the stress resultants and from the concentrated forces, was performed and this is shown in Figure 6. The difference between the distributions of the flap moments is of the order of 11% at the root section and gradually decreases to zero at 15m from the root (middle span of the blade). The result shows that the use of load time series overestimate the design load values leading to conservatism. Yet, the two lines of Figure 6 are much dependent on the fitting to the local maxima and the extrapolation performed. That means that the two curves could overlap by just selecting lower threshold values in the peak over threshold method of picking extreme values.

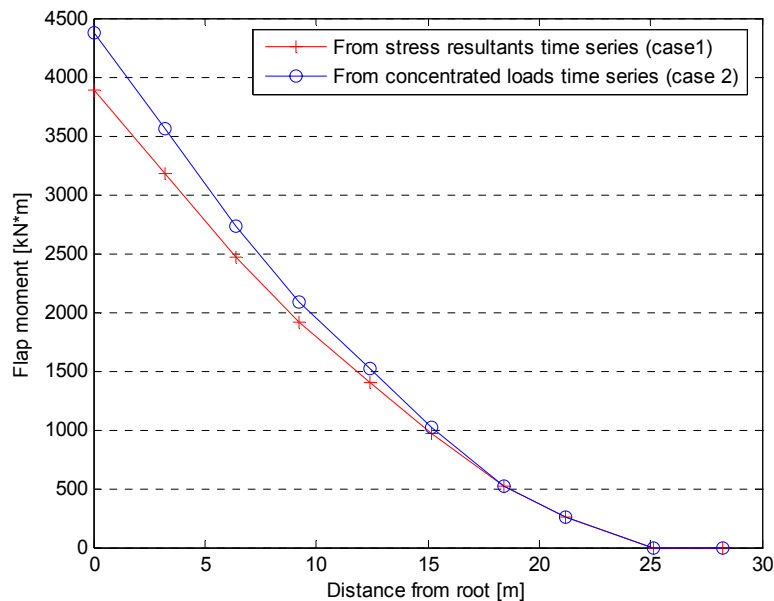


**Figure 6: Comparison of the flap moments produced through stress resultant time series and through concentrated forces time series**

## 4. Probability of failure

### 4.1 Lamina failure probability

The following discussion on the lamina (layer) failure is based considering a unidirectional off-axis layer under general in-plane loading as shown in Figure 7. For the failure prediction of composite laminates when subjected to a complex stress state a number of theoretical criteria can be used [39]-[41]. GL [12] and DNV-OS-J102 [13], for the composite materials propose the use of failure criteria on the layer level differentiating between matrix and fibre failure. A recommended failure criterion, enabling the identification of failure mode is the Puck criterion [42], [43]. Nevertheless, without loss of generality and following the discussion in [44], within the current work the failure criterion used is the quadratic version of the failure tensor polynomial in the principal material coordinate system, derived by Tsai and Hahn (TH) in [10]:

$$\frac{\sigma_1^2}{X_T X_C} + \frac{\sigma_2^2}{Y_T Y_C} + \frac{\sigma_6^2}{S^2} - \frac{\sigma_1 \sigma_2}{\sqrt{X_T X_C Y_T Y_C}} + \left( \frac{1}{X_T} - \frac{1}{X_C} \right) \sigma_1 + \left( \frac{1}{Y_T} - \frac{1}{Y_C} \right) \sigma_2 - 1 \leq 0 \quad \text{Eq. 4}$$

Denoting the left hand side of the inequality as  $K(\mathbf{X}, \boldsymbol{\sigma})$  then failure is assumed if:

$$K(\mathbf{X}, \boldsymbol{\sigma}) > 0 \quad \text{Eq. 5}$$

The probability of failure of the layer,  $P_F$ , is expressed by  $P_F = P(K > 0)$ .

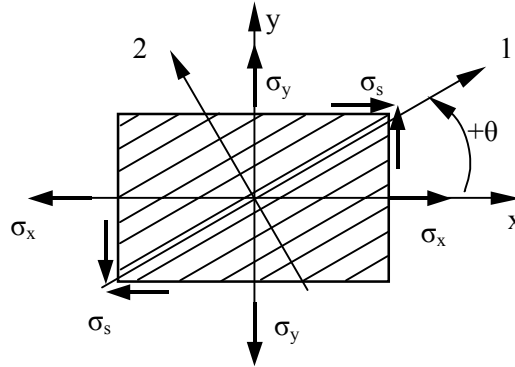


**Figure 7 Coordinate system for an off-axis unidirectional layer**

For a reliability based prediction of structural failure, numerical as well as analytical methods may be used, all of which tend to serve as an approximation of the joint probability integral of the appropriate failure function.

### 4.2 Laminate failure probability

A laminate can be modelled as a system of many components (layers), each one of them characterized by its own failure function, as described in the previous section. The failure of the laminate may in turn be characterized either by the failure of the first ply (FPF) or by the total failure, that is the successive failure of all layers in the laminate up to the failure of the last ply (LPF). In the current work, the failure of the laminate is considered to be characterized by the FPF method for two reasons. The first is that for the LPF prediction assumptions for the material degradation factors are needed during the estimation of the failure load. However, since there are a lot of discussions concerning the adequate degradation methodology including the

material degradation factors, as for example in [45] and [46], while the most usual way of determining this degradation methodology is to verify the assumptions with experimental results, the choice of a methodology would incorporate larger uncertainty in the reliability estimation, this way masking the results of the current work. The second reason is that although the FPF assumption underestimates the final failure of the laminate, this assumption constitutes a conservative albeit safe approach during the design of composite material structures as wind turbine blades.

Since the design is considered to be performed based on the FPF methodology, the analysis of a series system will result to the probability of failure of the laminate. Theoretically, the probability the system to be in a safe state is expressed by the spatial integral:

$$P_S = \int_{(\overline{A_1} \cap \overline{A_2} \cap \dots \cap \overline{A_n})} \dots \int f_{X_1, X_2, \dots, X_k} dX_1 dX_2 \dots dX_k \quad \text{Eq. 6}$$

where  $f_{X_1, X_2, \dots, X_k}$  is the joint probability distribution of the failure condition of the system,  $\overline{A_i}$  is the safe event that layer  $i$  ( $i = 1, 2, \dots, n$ ) does not fail and  $X_i$  ( $i = 1, 2, \dots, n$ ) are the stochastic variables of the problem.

The calculation of this probability or the respective probability of failure of a laminate through the above spatial integral is in general difficult. In most of the cases, approximate solutions are necessary. From this point of view, it would be also useful to have the respective probability limits. The limits for the failure probability of the laminate, where it is assumed that the failures of the layers are positively correlated are given by [47]:

$$\max_i P_{f_i} \leq P_F \leq 1 - \prod_{i=1}^k (1 - P_{f_i}) \quad \text{Eq. 7}$$

The range between the upper and the lower limit is dependent by the number of layers and the relative values of their probabilities. It should be noted that in the case of composite materials, the independent modes of failure are equal to the number of layers in the laminate, if each layer is characterized by its own failure function (as described in former sections of the current document).

Specifically, in the case that the failures of the layers in the laminate are positively correlated, the probability of failure of the laminate is given by following equation:

$$P_F = \max_i P_{f_i} \quad \text{Eq. 8}$$

In the case where a more narrow estimation of the failure probability limits for the laminate is sought, the correlation coefficient between the failures of the layers should be determined. However, the correlation coefficient, alike the degradation factors, is difficult to be estimated, since the degree of correlation of the layer properties in a laminate depends for example by the manufacturing procedure of the laminate, the spatial distribution of the fabric properties and the lamination sequence. In particular, for similar layers it can be assumed that the more standardized manufacturing procedure the more the positive correlation of the layer properties.

Thus, to simplify the analysis conducted and without loss of generality it is assumed that the failure probability of the laminate can be approximated by the maximum failure probability estimated in any layer of the lamination sequence, assuming that the laminate is a series system and that a positive correlation exists on the behaviour of the layers in the sequence. Therefore, the purpose of the analysis is to determine the cumulative distribution function

(CDF),  $F_K(K)$ , of the failure condition,  $K(\mathbf{X}, \boldsymbol{\sigma})$  of each layer in the laminate, and then define the failure condition of the laminated composite.

### 4.3 Failure probability of the blade section

Since we are studying the failure of a composite material rotor blade, more specifically, a multi-cellular thin walled heterogeneous section made of fibre reinforced laminates, the meaning of “blade section failure” should be defined as well. Similar to the line of thinking followed for the determination of failure of the laminate, the section of the blade in this work is considered as a series systems. That is, failure of any of the elements in the blade section is assumed to result in failure of the section. Moreover, the failures of the elements in the section are assumed to be positively correlated.

Therefore, it is assumed that the failure probability of the section can be approximated by the maximum failure probability estimated in any element (laminated substructure) of the section, assuming that the section is a series system and that a positive correlation exists on the behaviour of the elements in the sequence. This is well supported by the fact that for similar elements a more standardized manufacturing procedure results in a more positive correlation of the element properties.

## 5. Probabilistic methods

There several available general software codes for the estimation of structural reliability. Their number is continuously increasing, following the increase in structural applications requiring reliability estimations. A review of available general purpose software for structural reliability estimations can be found in [48]. Most of them are based on approximating methods, mainly first (and second) order reliability methods, as an alternative to simulation-based methods, meaning iteratively sampling the solution, such as the Monte Carlo simulation and enhancements thereof. Many, such as ANSYS have also available the response surface method.

However, the failure functions applicable to composite materials result in multi-modal limit states [49]. In such applications, combining these failure functions with the first order reliability methods makes it not certain that the global minimum will be obtained. Therefore, the method does not always yield accurate results, overestimating or underestimating the reliability of the structure, depending on the loading case and the structure itself [50]. In other cases, the First order reliability method failed to converge for all combinations of applied stresses and lay-ups as applied in [27]. Furthermore, in the review of available general purpose software for structural reliability estimations [48], it is pointed out that the developers of packages relying in approximate methods, such as PROBAN and STRUREL, offer and recommend the use of simulation methods to verify the accuracy of the approximate estimate. Moreover, among the conclusions of the same review [48], is that the probabilistic models used for the presentation of the applicability of the various software programs consisted of a rather small number of variables and the level of the failure probability was rather large. The structural analysis of a rotor blade, however, involves not only a large number of variables, but covers the range from very small to relatively small reliability levels.

Within the work of WP3 of UPWIND one of the available software for the structural reliability estimation, Response Surface Method of commercial finite element analysis package ANSYS, was implemented for the analysis of the wind turbine blade as will be described in following sections. Yet, during the application a lot of challenges were encountered, especially considering that the application should be suitable to be used during the design phase of blade. These will be also discussed. Therefore, it can be seen that the use of composite materials in

the blade structure and the many stochastic variables that are thus involved in the analysis along with the higher complexity of the existing probabilistic methods makes the available reliability estimation methods not attractive for integration in the design procedure, where a large number of loading cases has to be checked against a number of alternatives in terms of structural properties.

To overcome this, an already developed numerical procedure for determining strength of a composite laminate, using various suitable failure criteria, by taking into account the stochastic nature of anisotropic (strength and stiffness) material properties is implemented in appropriate software routines in the form of pre- and post-processor that can be used along with current aero-elastic codes. The analysis of the blade structure is performed considering multi-cellular thin walled heterogeneous sections made of fibre reinforced laminates, taking into account the in-homogeneity and the elastic anisotropy of the cross sectional elements. Along with the mechanical normal and shear stresses due to the applied loads, the hygro-thermal stresses, due to temperature differences and moisture concentration can also be computed. The reliability estimation for each laminate is conducted either by employing the Edgeworth expansion technique or the Response Surface Methodology, at the layer level. Not only the strength properties of the material are considered as stochastic parameters of the model but also the variability of the elastic and thermo-mechanical properties of each layer in the lamination sequence is taken into account. This leads in quantifying blade design reliability.

## 5.1 Response Surface Method (RSM)

Response surface method (RSM) has a long history and nowadays has many applications in the field of engineering, in process optimization and in structural reliability. In the developed methodology RSM is used combined with MC.

RSM is applied herein as a technique of constructing an approximate model either of the FE rotor blade model (when ANSYS 3-D finite element model is used) or of the THIN solution (when sectional analysis of the blade is performed). That is, instead of repeatedly solving through THIN or through the time consuming FE procedure, respectively, approximation (regression) models are formed and a great number of simulations are performed in combination with MC to estimate the reliability.

The typical RSM involves central composite design (CCD) for the design of experiment (DoE), second order polynomial models with or without cross terms, regression analysis and testing of model accuracy.

DoE provides the appropriate sample points that are used for a limited number (few hundreds) of experiments, i.e. solving repetitions (THIN or finite elements) to fit the regression models. The selection of the proper design depends on many factors. For a second order polynomial regression model, CCD is the most appropriate DoE. It is composed of three different designs. It consists of a full or fractional (resolution V) two-level factorial design [16]. There are also axial and centre points. CCD is performed for all input variables considered as random variables in the problem. The engineering elastic constants  $E_1$ ,  $E_2$ ,  $\nu_{12}$ ,  $G_{12}$  of the material properties and the loads are taken as random variables in the cases studied herein. For the case of the FE analysis (presented in [19]) the loads, were the three concentrated forces applied along the blade length, while for the case of THIN analysis the stochastic loads were the stress resultants ( $N_x$ ,  $N_y$ ,  $N_z$ ,  $M_x$ ,  $M_z$ ,  $M_y$ ) of the section. The number of simulations depends on the number of random (input) variables. For example, in [19] for 7 input variables, 79 FE analyses were required, while for the 10 input variable within THIN, 149 iterative analyses are required.

Each random variable has five levels where it is tested (two factorial points, two axial points and one centre point). These levels are defined in a way to give a circumscribed CCD with the axial point to be at the 0.005 and 0.995 percentiles for every random variable. When the appropriate

sample points are obtained through DoE, a regression analysis is implemented to estimate the unknown coefficients of the approximation models (second order polynomials with cross terms):

$$y = b_0 + \sum_{j=1}^k b_j X_j + \sum_{j=1}^k b_{jj} X_j^2 + \sum_{j=1}^k b_{jj} X_i X_j \quad \text{Eq. 9}$$

Various statistical tests are commonly used to validate the regression models: F-test, coefficient of determination R and residual checking. However, since the “experiments” are computational, in the absence of any random error only the visual checking of the residual and the coefficient of determination could be helpful [51], [52].

It must be said that RSM is used here for the derivation of approximate models for the in-plane strains ( $\varepsilon_x$ ,  $\varepsilon_y$ ,  $\varepsilon_s$ ) developed at any ply of any element in the blade. The main difference with the common application of RSM in the field of structural reliability [53], [54] is that it was not attempted to approximate the limit state function with a polynomial model because the analytical expression of the state function was already known, i.e. Eq.4. For the purposes of the present analysis, a regression model to calculate the strain components was foreseen to avoid the time consuming FE or THIN solution repetitions.

Due to ANSYS code limitations (supporting up to 5,000 random variables), CCD was performed only for the upper and the lower layer of every element. A FORTRAN routine was implemented to complete the task taking advantage of the linear distribution of the strain components through the thickness of the element. Regression analysis and Monte Carlo were also implemented in an external FORTRAN routine. Thus, the output parameters for the FE implementation were the three in-plane strains ( $\varepsilon_x$ ,  $\varepsilon_y$ ,  $\varepsilon_s$ ) of the ply.

For the implementation with THIN, approximate models of the in-plane strains were developed at the top of the upper and the bottom of the lower plies for each node of any element in the section of interest. That is, for every node six regression models are constructed. For the in-between plies, a linear distribution of the strain was assumed through the thickness of the element. Therefore, the output parameters for the sectional implementation were the six in-plane strains of the ply (upper and lower).

Finally, after the definition of the regression models, MC, implemented as described in section 5.3, was executed for a sample of 2,000,000 values. The only difference is that the strains are calculated through the regression models instead of FE or THIN solutions, respectively, thus increasing the speed of the procedure by a factor of at least 4.

## 5.2 Edgeworth Expansion Method (EDW)

The analytic approximation featuring functional expansion techniques was used in [55] to predict the cumulative distribution function of failure under uniaxial tension in off-axis composite coupons. This method was further developed by the authors in [56] and [57] for the general plane stress case of a composite layer and of a laminate, respectively, considering the strength properties as stochastic variables, while in [28] the method was further enhanced to include the stochastic nature of the elastic material properties for the case of a laminate.

The method introduced by Edgeworth uses a series expansion of the normal cumulative distribution function (CDF), denoted  $\Phi(K)$ , to approximate an unknown CDF in terms of central moments of the random variable,  $K$ . This is given by [58]:

$$\begin{aligned}
F_K(K) &= \Phi(K) \\
&- \frac{1}{3!} \frac{\mu_3}{\mu_2^{3/2}} \Phi^{(3)}(K) \\
&+ \frac{1}{4!} \left( \frac{\mu_4}{\mu_2^2} - 3 \right) \Phi^{(4)}(K) + \frac{10}{6!} \left( \frac{\mu_3}{\mu_2^{3/2}} \right)^2 \Phi^{(6)}(K) \\
&- \dots
\end{aligned} \tag{Eq. 10}$$

where,  $\Phi^{(n)}(K)$  is the n-th derivative of the normal CDF and  $\mu_i$  are the central moments of the failure function. Each line of Eq.10 represents one term of the series, i.e. the first three terms are shown. In [57] and [28] it was shown that, for the CDF of the failure condition the use of only two or three terms for better accuracy of the small values of failure probability, which of course are of interest, is sufficient. The probability of survival, or reliability, is given by  $F_K(0) = P(K \leq 0)$ .

The moments of the failure function are calculated employing the method of moments, resulting in the following equations, for the mean value,  $E(K)$ , variance,  $\mu_2$  and 3<sup>rd</sup> central moment,  $\mu_3$ , respectively:

$$E(K) = \bar{K} + \frac{1}{2} \sum_{i=1}^M \left( \frac{\partial^2 K}{\partial x_i^2} \right) \mu_{2,i} \tag{Eq. 11}$$

$$\mu_2 = \sum_{i=1}^M \left( \frac{\partial K}{\partial x_i} \right)^2 \mu_{2,i} + \sum_{i=1}^M \left( \frac{\partial K}{\partial x_i} \right) \left( \frac{\partial^2 K}{\partial x_i^2} \right) \mu_{3,i} \tag{Eq. 12}$$

$$\mu_3 = \sum_{i=1}^M \left( \frac{\partial K}{\partial x_i} \right)^3 \mu_{3,i} \tag{Eq. 13}$$

where  $\bar{K}$  is the value of the failure function when the mean values of each basic variable,  $x_i$ , of the problem are employed, i.e. the strength and elasticity material (layer) properties,  $\mu_{2,i}$  and  $\mu_{3,i}$  are the 2<sup>nd</sup> and 3<sup>rd</sup> central moment of the variables, respectively, while  $M$  is the number of independent variables in the problem. It must be noted that all derivatives are evaluated at the mean values of the basic variables.

Edgeworth Expansion method, is thus, formulated in terms of the failure function's moments, which in turn are calculated using the moments of the individual strength distributions, known by experiment in the case where the elastic properties of the composite are considered to be deterministic. In case that the elastic properties variability is also taken into account, then the applied stress on the layer level is dependent on the stochastic variables of stiffness. By use of partial differentiation one can derive the partial derivatives needed for the evaluation of the moments of the failure function.

### 5.3 Monte Carlo method

In the present work, direct Monte Carlo simulation is implied for all cases. That is, samples of all random variables are generated using appropriate random number generators and repetitive

simulations are performed. The probability of failure is determined as the ratio of the number of times in which the failure in the layer was detected to the total number of trials, that is:

$$P_{F_i} = n_{F_i} / n_{tot} \quad \text{Eq. 14}$$

where  $n_{F_i}$  is the times that failure was detected for layer  $i$  and  $n_{tot}$  is the number of simulation repetitions.

The number of repetitions necessary for convergence of the simulation prediction was taken empirically equal to  $100/P_F$  [59], where  $P_F$  is the expected probability of failure. This is a good approximation for failure probabilities of the order  $10^{-4}$  and coefficient of variation of the estimated probability not lower than 10% [60].

Moreover, it should be noted that since during the MC simulation performed random number generation was conducted for a number of variables rather than a single variable, the random number generators used in this application were extensively checked for inconsistencies according to statistical tests described in [61].

Additionally, for the load random variables, following a Gumbel distribution and being correlated, special care was taken. To take this into account, a Random Number Generator for correlated Gumbel variables was adopted, that has been previously introduced for correlated Normal variates [60]. The method implements the principal component analysis of the covariance matrix of the correlated variables. The statistical features of the generated samples were found in excellent agreement with those of the initial distributions.

## 6. Examples and discussion

GL [12], DNV [13] as well as IEC 61400-1 [11], followed for the blade design dictate an analysis using partial safety factors. These are to be applied on the loads, to cover loading uncertainties and to material properties, covering not only uncertainties and variability of the properties per se, but also geometric, environmental and other uncertainties that are not taken directly into account. Yet, at least for the partial safety factors applied on the material properties there are differences between the various design guidelines and standards. Differences between deterministic design (focusing on the subject of materials) were discussed in [28] and later in [27] for the case of laminates. In this section the discussion will be extended to sections of the blade and the blade model.

The potential of the developed methodologies are demonstrated through examples presented for the blade response under extreme loading. Initially, an example carefully selected is presented in order to evaluate a number of different reliability levels over the cross-section as well as the effect of the variability in material strength and elasticity, and finally loads on the reliability of the section. Results are compared with corresponding ones from Monte Carlo simulations and are found in good agreement. Following that, the application of the Response Surface Method on the 3-D shell finite element model of the blade is discussed. Finally, RSM and EDW methodologies applied in combination with the sectional analysis tool THIN are compared with direct Monte Carlo simulation results.

### 6.1 Effect of variability in strength, elasticity and loads in blade reliability (EDW, MC)

The application of the EDW methodology developed within the frame of UPWIND WP3 was presented in [23]. In this section only the results will be discussed in detail. For the assessment of the developed methodology based on the EDW as an example a typical aerodynamic

section, with the corresponding lamination sequences, as shown in Figure 1 was selected. The material properties for the UD layer, employed were taken from [29] and are shown in Table 2. For the bi-directional layer used, since no statistical information were available, it was assumed that it is formed as a [+45/-45] sub-laminate of off-axis UD layers, however, the thickness of each layer is about the 1/3 of the UD layer, yet the material properties for these layers was treated as independent from the material properties of the UD layers. Moreover, for the structural foam used in the trailing edge and the shear webs on the section the mean values of the properties were taken from [62], while the density variation was assumed to drive the variation of the strength and elasticity properties of the foam. The mean values, the standard deviation and the coefficient of variation of the structural foam are presented in Table 3. The variables were assumed to follow the normal distribution, although other distributions could be used as well, e.g. Weibull, Lognormal, etc.

**Table 2: Material properties and statistical parameters of UD layer**

| Property       | Mean Value | St. Deviation | C.O.V. (%) | Distribution |
|----------------|------------|---------------|------------|--------------|
| $E_1$ (GPa)    | 39.04      | 1.032         | 2.64       | Normal       |
| $E_2$ (GPa)    | 14.08      | 0.325         | 2.31       | Normal       |
| $G_{12}$ (GPa) | 4.24       | 0.099         | 2.34       | Normal       |
| $\nu_{12}$     | 0.291      | 0.0271        | 9.34       | Normal       |
| $X_T$ (MPa)    | 776.50     | 36.143        | 4.65       | Normal       |
| $X_C$ (MPa)    | 521.82     | 16.500        | 3.16       | Normal       |
| $Y_T$ (MPa)    | 53.95      | 2.576         | 4.78       | Normal       |
| $Y_C$ (MPa)    | 165.00     | 4.849         | 2.94       | Normal       |
| $S$ (MPa)      | 56.08      | 1.119         | 2.00       | Normal       |
| $h$ (mm)       | 0.938      | -             | -          | -            |

**Table 3: Material properties and statistical parameters of structural foam**

| Property    | Mean Value | St. Deviation | C.O.V. (%) | Distribution |
|-------------|------------|---------------|------------|--------------|
| $E$ (MPa)   | 75.0       | 9.00          | 12.00      | Normal       |
| $G$ (GPa)   | 20.0       | 1.00          | 5.00       | Normal       |
| $\nu$       | 0.420      | 0.0450        | 10.71      | Normal       |
| $X_T$ (MPa) | 1.800      | 0.150         | 8.33       | Normal       |
| $X_C$ (MPa) | 1.000      | 0.075         | 7.50       | Normal       |
| $S$ (MPa)   | 0.900      | 0.075         | 8.33       | Normal       |
| $h$ (mm)    | 10.000     | -             | -          | -            |

In Figure 8 the node numbering used on the section is shown. Also, by the different symbols an indication of the changes in the lamination sequences is shown. Element numbers, which are not shown on the sketch, start at 1 for the element connecting nodes 1 and 2, and continuing in sequential order for the elements around the section to element number 160 connecting nodes 160 and 1. Then, the elements on the shear web are numbered starting with the one nearest the trailing edge of the blade, with element number 161 corresponding to the element connecting nodes 25 and 167 and element number 168 connecting nodes 161 and 137. The elements of the shear web nearest the leading edge of the blade start with element 169 connecting nodes 57 and 174 to element 176 connecting nodes 168 and 105.

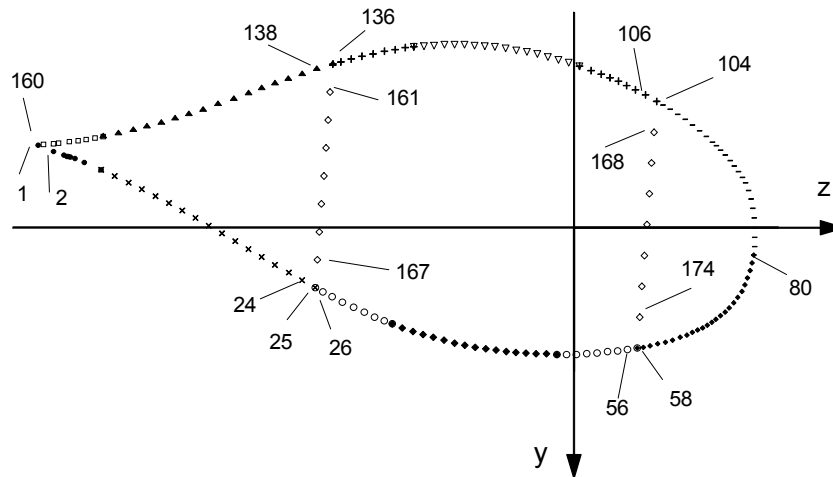


**Figure 8 Nodes numbering at section**

In order to be able to compare the effectiveness and accuracy of the Edgeworth Expansion technique employed, the section was designed so that from node to node, failure at various probability levels is captured. Of course, with this condition the overall result for the section is failure (with probability of failure equal to 1).

In Figure 9 results are presented for the case of the section when only the strength properties are assumed to be stochastic. Comparison between the MC simulation and the Edgeworth Expansion technique data shows that the two methods are in good agreement. At this point it should be mentioned that the time needed for the MC simulation (incorporating 2 million repetitions) is about 24 hours while the Edgeworth Expansion does not take much longer than a purely deterministic analysis, with results obtained within less than 10 seconds.

In the same figure also the deterministic results concerning reserve factor values,  $R$ , and not probability of failure are plotted against the right hand vertical axis. Calculations were performed with the mean values of the strength properties, not taking into account any partial safety factors. It should be noted, that for the deterministic reserve factor,  $R$ , failure is assumed if  $R < 1$ . Moreover, emphasis should be put on the fact that the reserve factor presented as the deterministic result cannot be connected to the reliability level of the structure. For the example presented herein, the reserve factor in the range from 1 to 1.3 corresponds to probability of failure ranging from 0.5 to  $1.5E-6$ , as derived through the MC simulation. Thus, failure is predicted for elements on the tension side of the blade on the elements mainly on the central part of the side (spar cups), but also for some elements on the trailing edge side of the section close to the shear web. However, it should be reminded that this is not a properly designed section to withstand loading, but rather the section and the loading were modified so that predictions for various probability levels would be possible among the elements on the section.

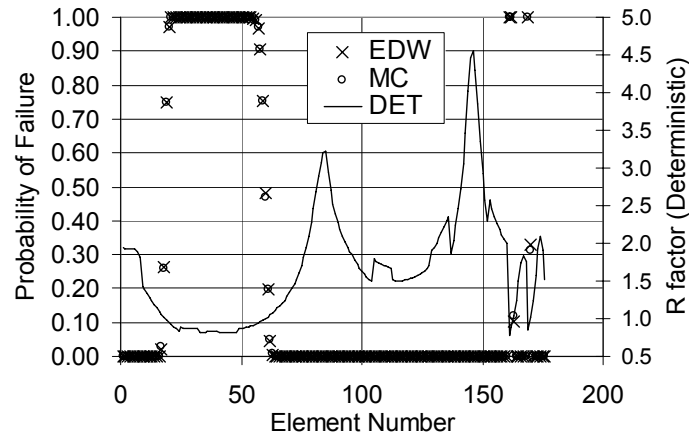


**Figure 9 Element results where only the strength properties are assumed stochastic**

In Figure 10 results are presented for the case where both the elastic and strength properties of the material are assumed to be stochastic. Again the results of the Edgeworth Expansion Technique are in good agreement with that of the MC simulation. The extension “-EL” in the legend denotes that apart from the strength properties of the material, also the elastic properties are assumed stochastic.

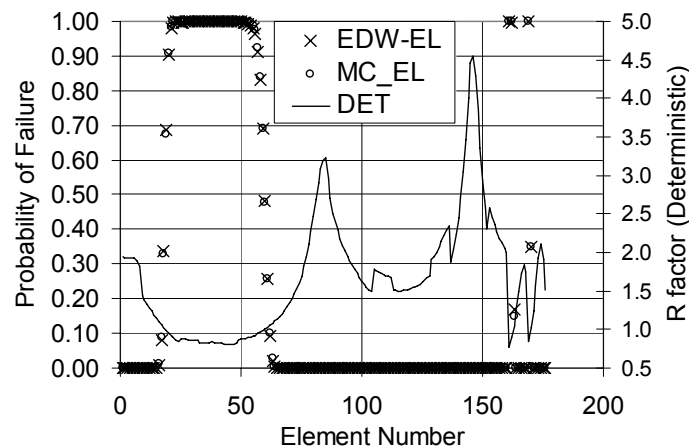


**Figure 10 Element results when strength and elasticity properties are assumed stochastic**

The effect of incorporating the elastic material properties variability is better seen in Figure 11, where the results of the MC simulation are shown for the case where only the strength properties are assumed stochastic, shown by circles, denoted “MC”, and for the case where both strength and elastic material properties are assumed stochastic, shown by crosses, denoted “MC-EL”. By noticing the elements for which failure probability is less than 0.5, which are of interest, it can be seen that neglecting the variability of the elastic properties leads to an overestimation of the reliability of the structure. The opposite is observed for elements with probabilities of failure higher than 0.5. That is, taking into account the variability of elastic material properties the probability of failure predicted is less than that estimated by considering only the variability of the material strength properties.

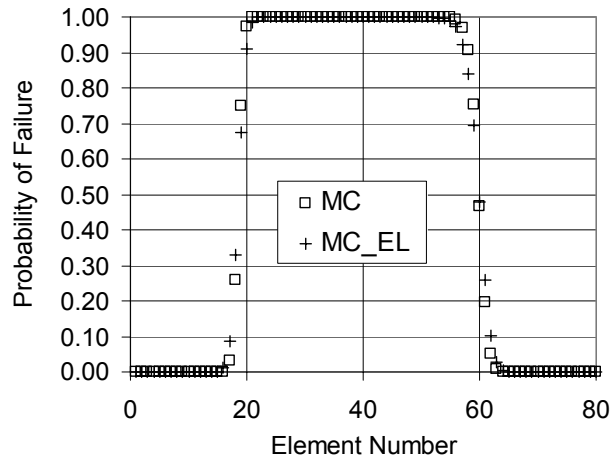


**Figure 11 Effect of Elasticity variability on element results (MC method)**

It should be noted, however, that the variation of the UD layer mechanical properties is considered as relatively low, due to the fact that the experimental data used for the statistical analysis (as this was presented in [29]) incorporate test results from a single plate, thus eliminating the variability between material (resin and fibres) batches that should be considered during the usual structural design procedure of the blade. This fact is also expected to affect the results presented for probability of failure of the section, when the variability of the material elastic properties is included in the analysis.

A side result of the currently presented analysis is the estimation of the variability of the sectional properties, when the variability of the material elastic properties is taken into account. For the presented case, the mean value and the coefficient of variation of the sectional properties, as derived through the MC simulation (by 2 million repetitions) and the Edgeworth Expansion analysis is shown in Table 4. Again the obtained results are in good agreement, with the analytic results showing a little less variation than the MC ones.

**Table 4: Sectional properties and variation**

| Property                     | MC         |            | EDW        |            |
|------------------------------|------------|------------|------------|------------|
|                              | Mean Value | C.O.V. (%) | Mean Value | C.O.V. (%) |
| EA (N)                       | 1.52E9     | 2.51       | 1.50E9     | 2.38       |
| $EI_Y$ (Nm <sup>2</sup> )    | 1.29E8     | 2.38       | 1.30E8     | 2.26       |
| $EI_Z$ (Nm <sup>2</sup> )    | 4.78E7     | 2.48       | 4.77E7     | 2.45       |
| $EI_{YZ}$ (Nm <sup>2</sup> ) | 7.99E6     | 2.18       | 7.98E6     | 2.15       |
| GJ (Nm <sup>2</sup> )        | 1.69E7     | 1.73       | 1.69E7     | 1.43       |

These results can be used in combination with aero-elastic codes, for estimation of the effect of the material property variability in the predicted wind turbine behaviour and loading of the various mechanical components, including the blade. Additionally, the results might potentially be used in a probabilistic assessment of the global buckling of the blade.

### 6.1.1 Introducing loading variability

For the estimation of the effect of the stochastic character of applied load on the strength of the blade, the numerical tool was accordingly enhanced to enable the introduction of load variability.

Similar to the introduction of the material properties variability, for incorporating the load as a stochastic variable the statistical characterization of the internal resultant axial and shear forces,  $N$ ,  $Q_y$  and  $Q_z$ , respectively and the internal resultant bending and torsional moments,  $M_z$ ,  $M_y$  and  $M_x$ , respectively, at each selected section across the length of the blade. These internal resultants are used as input parameters in the THIN module for the more detailed stress analysis on the blade section.

For modeling the variability of the loading on the section the procedure presented in 3.2 should be employed. Yet, for the assessment of the methodology developed, as an example, two load cases having the same mean value as in the previous examples, where the variability was neglected but with different variation for each case, were assumed. In Table 5 the statistical parameters of the internal resultant force and moment components are shown, that were used for the examples presented in the present work. In this table the coefficient of variation for the torsional moment ( $M_x$ ) is not given, since it is assumed that the component has a zero mean. Without loss of generality, regarding the statistical distribution type, the internal resultant forces and moments are assumed to follow the Normal distribution. Based on the parameters presented in Table 5 the third and fourth moment were calculated for the EDW method, while for the Monte Carlo application the standard deviation was used.

**Table 5:** Statistical characteristics of the internal resultants forces and moments on the blade section

| Component   | Mean Value | Case 1<br>(Large variation) |            | Case 2<br>(average variation) |            |
|-------------|------------|-----------------------------|------------|-------------------------------|------------|
|             |            | Standard Deviation          | C.O.V. (%) | Standard Deviation            | C.O.V. (%) |
| N (kN)      | 452.416    | 0.905                       | 0.2        | 0.905                         | 0.2        |
| $Q_y$ (kN)  | 278.391    | 46.390                      | 16.7       | 13.928                        | 5.0        |
| $Q_z$ (kN)  | -73.184    | 146.287                     | 200.0      | 7.348                         | 10.0       |
| $M_z$ (kNm) | 1529.867   | 254.971                     | 16.7       | 76.485                        | 5.0        |
| $M_y$ (kNm) | -399.311   | 798.622                     | 200.0      | 39.931                        | 10.0       |
| $M_x$ (Nm)  | 0.000      | 10.000                      | -          | 10.000                        | -          |

As an example in Figure 12 results of the EDW method are compared with MC simulation results for the mean (in-plane) axial stress resultant,  $N_x$ , divided by the thickness of the respective laminate,  $h$ , for each element on the section for load case 1 (having large variation). For the MC simulation 180,000 samples have been used. The results of both methods are identical. The same is true for the estimation of the mean shear stress resultant, which is not presented on the figure for clarity purposes.

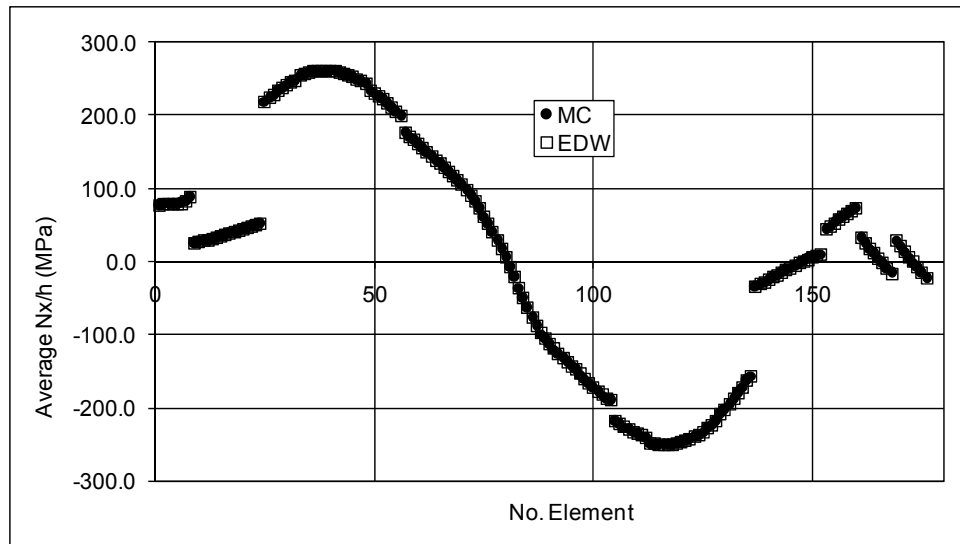


**Figure 12 Mean values of the axial stress resultant,  $N_x$ , on the section elements ( $h$  the total thickness of each laminate) by the MC and EDW methods.**

Respectively, in Figure 13 the estimation results of the standard deviation of the shear stress resultant, divided with the laminate total thickness for the section elements for the same load cases. In the same figure also the percent difference between the MC estimation and the EDW results is shown, denoted as diff, on the right hand vertical axis. The difference is smaller than 0.5% for the estimation of the standard deviation in all section elements. Similar results have been found for the axial stress resultant on the elements.

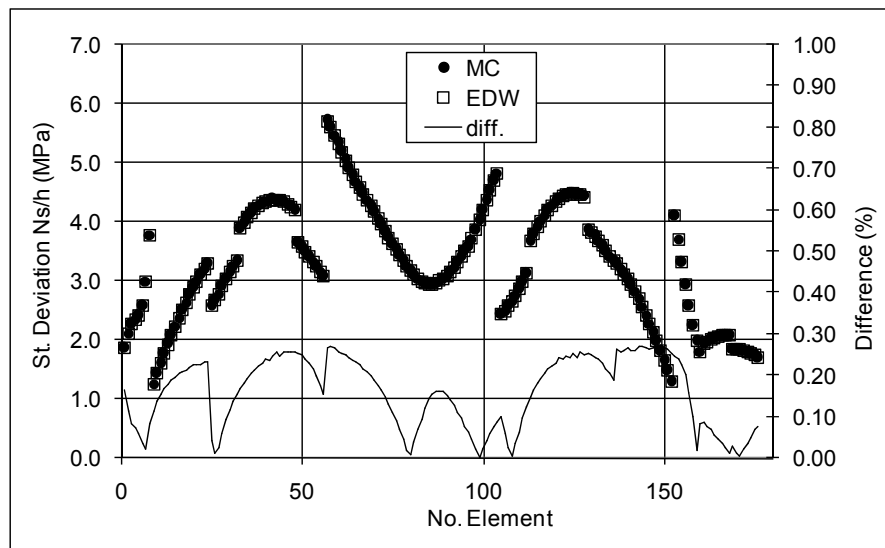


**Figure 13 Standard deviation of the shear stress resultant,  $N_s$ , on the section elements ( $h$  the total thickness of each laminate) by the MC and EDW methods and percent difference (diff.).**

In Figure 14 the effect of load variability on the failure probability of the section elements is presented (for load case 1) using the Monte Carlo and EDW methods, in comparison with the case where the load variability is neglected. In the area of interest, that is for the cases where the failure probability of the elements was small when load variability was neglected (elements 1... 16 and 64... 160), a significant increase on the failure probability is observed when taking into account the load variation. It should be noted however, that the load variability assumed for this case can be characterized as very large.

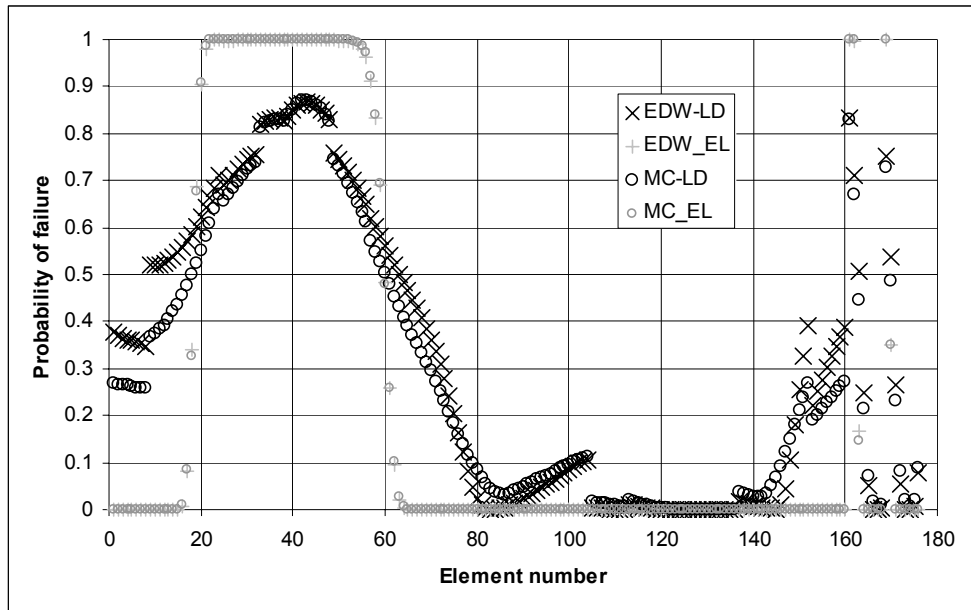


**Figure 14 Element failure probability by the MC and EDW methods when load variability is neglected (-EL) and when load variability is taken into account (-LD).**

To make this more clear, in Figure 15 the effect of the magnitude of load variability on the element failure probability is presented. The load case shown include the case with zero load variability, denoted EDW-no variance, the case where a medium variation was assumed (load case 2), denoted as EDW-low variance, and the case where the variation is large, as presented in the above, denoted EDW-high variance.

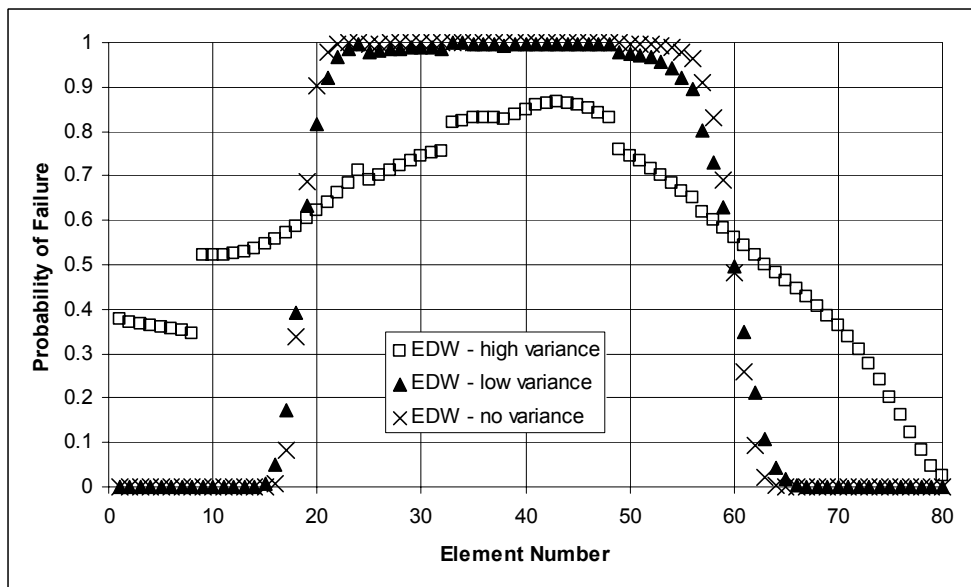


**Figure 15 Effect of magnitude of load variability on the element failure probability by EDW method for three cases (no variance: deterministic load case, low variance and high variance)**

Finally, it should be mentioned that for the results of these two cases examined for one section of the blade 24 hours for the Monte Carlo simulation were necessary (on an average commercial PC station), while only a few seconds for the analytic EDW method.

The accuracy of the EDW method (in the prediction of the failure probability) is rather average for low probability cases of interest. Yet, if one considers the particularly high computational cost of the “accurate” Monte Carlo method in addition with the calculation time needed for the result of only one section, the advantage of the analytic method is evident. This advantage makes the method even more attractive during the design of a blade, where a lot of trial cases are required, so as to approach an optimum solution. Therefore, a more expensive but accurate method could be used only for the verification of the design during a final stage.

## 6.2 RSM and Finite Element Model Application

The application of the Response Surface Method on the 3-D shell finite element model of the blade was presented in [19]. The rotor blade was designed for ultimate strength according to the current edition of IEC 61400-1 [11]. The Tsai-Hahn failure criterion, Eq. 4, was calculated for all the layers, for all the elements in the blade. Its maximum values (over each element) are plotted as an example in Figure 16 for the suction side and Figure 17 for the shear webs. As it is observed almost no element fails except the a few elements (7 in total) located in the shear web from 14.15m to 15.5m from the root and in the trailing edge of the suction side from 16.58m up to 17.17m from the blade root with maximum failure criterion value of 1.048. The failed plies were of 90° fibre orientation and the failure criterion values were less than 1.048, very close to unity. Thus, according to the IEC 61400-1 ed.3 the rotor blade can be considered as properly designed for the load case applied.

### 6.2.1 Reliability analysis

Reliability analysis was performed taking into account the stochastic behaviour of the material properties and the concentrated loads acting on the blade, taking into account the relevant correlation matrix, as presented in previous sections of the current document. Probability of failure was calculated for every layer (top and bottom face) for every element and the maximum of each element is plotted Figure 18 for the suction side of the blade and Figure 19 for the shear webs. These views of the blade model are the same as those used for the presentation of the deterministic results for facilitating comparison.

The maximum failure probability, equal to 0.0182, was observed at the element #3591, 14.7m from the root in the shear web, having also the maximum deterministic failure criterion value. It corresponds to a ply with fibres oriented at 90°, i.e. transverse to the blade axis.

Low values of failure probability,  $P_F < 1 \cdot 10^{-4}$  were calculated for the inboard part of the blade, up to nine meters from the root. The skin of the blade as well as the two shear webs in the specific area can be considered safe enough.

The elements with red color,  $P_F > 1 \cdot 10^{-2}$ , are mainly located in the trailing edge and the outboard shear web. The plies with such probability values have fibres oriented either at 90°, especially for the shear webs, or at  $\pm 45^\circ$ .

The green,  $1 \cdot 10^{-3} < P_F < 1 \cdot 10^{-2}$ , and the cyan,  $1 \cdot 10^{-4} < P_F < 1 \cdot 10^{-3}$ , coloured elements correspond again to failure probabilities of 90° and  $\pm 45^\circ$  plies. They are located mainly in the central part and beyond 10m from the root of the blade, especially in the pressure side.

Finally, it was revealed that all plies with fibres oriented along the blade axis, i.e. 0°, had probability of failure values,  $P_F$ , not exceeding  $1 \cdot 10^{-4}$  independently of their position in the blade.

The ability of determining the failure probability of every ply in any layup of the rotor blade will trigger the discussion on the level of the acceptable probability and the associated modes of failure.

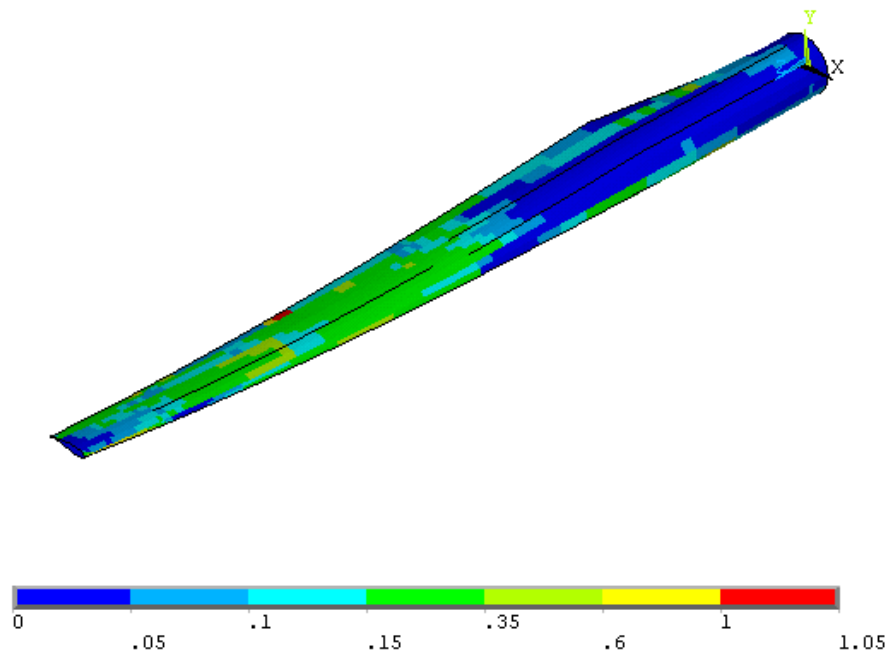


Figure 16: Tsai-Hahn failure criterion (suction side)

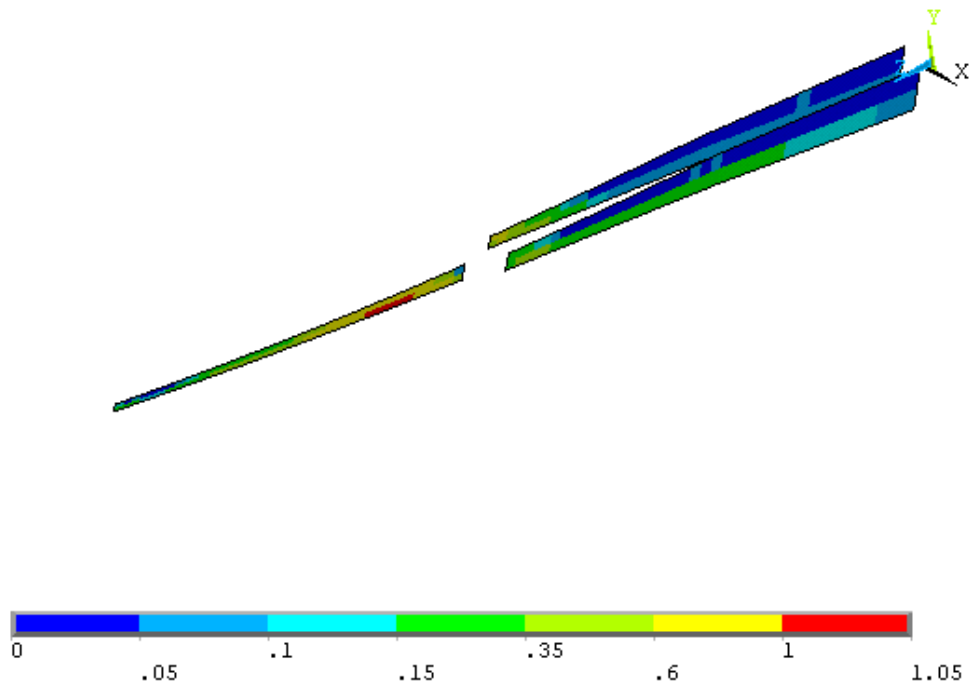


Figure 17: Tsai-Hahn failure criterion (shear webs)

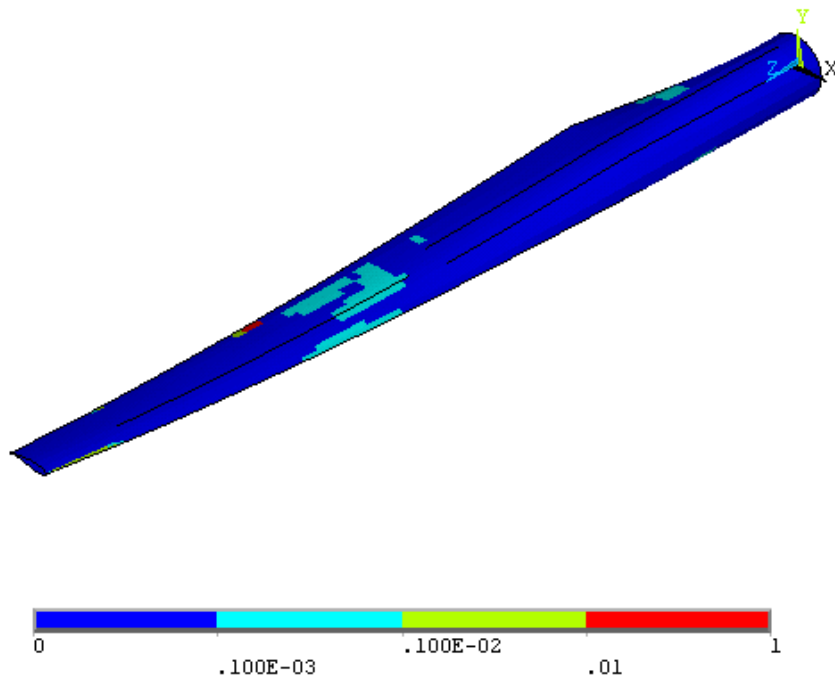


Figure 18: Failure probability contour plot (suction side)

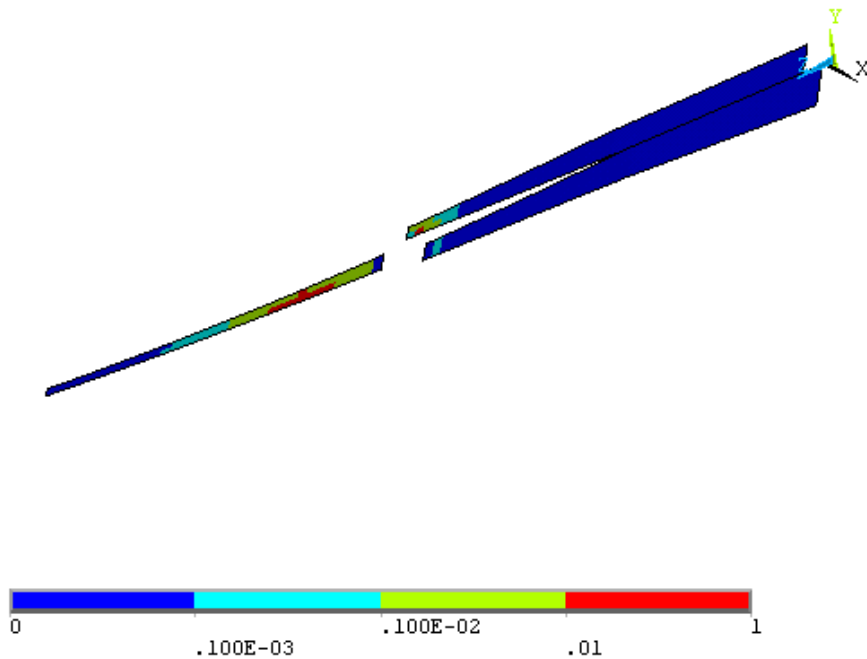


Figure 19: Failure probability contour plot (shear webs)

### 6.2.2 Validation of the result

The validation of the probabilistic procedure presented in this work can only be performed with a base simulation method, i.e. the direct Monte Carlo simulation. However, with the FE model of

a rotor blade, even with the coarse mesh used in this application, this is unrealistic: feasible but very expensive.

Two alternatives were implemented to enhance confidence on the results derived. First, the RSM combined with MC was validated in numerical models of simply supported unidirectional (UD) and multidirectional (MD) plates modelled in ANSYS, for which the performance of MC simulations was feasible. Extensively investigations of the RSM application in laminates lead to very good results.

The second technique was to run some FE iterations of the rotor blade model near the limit surface in the design space. From the input matrix of 2,000,000 rows, 455 samples were selected which were shown, through RSM models, to yield a value of the Tsai-Hahn criterion (Eq. 4) near unity (the limit state). The FE model of the blade was repeatedly solved for these 455 random values of material properties and loads, and the Tsai-Hahn failure criterion was evaluated for each ply and element of the rotor blade.

A specific element on the spar cap of the pressure skin of the blade was selected because its probability of failure was equal to  $1.22 \cdot 10^{-4}$  which is considered sufficiently small to test the accuracy of the RSM method. The element is located close to the middle span of the blade. The failure criterion values as calculated from the FE code and from the RSM models are plotted in Figure 20 where the 455 samples were sorted with respect to the RSM predictions.

The underlying principle is that for an accurate estimation of the failure probability, the regression models should correctly predict whether every simulation lies in the safe or the unsafe region. When for a sample point the results concerning failure from the FE solution and the RSM models contradict, then this is considered as a misplaced point. In Figure 20 the red line shows the limit condition (values greater than unity lie in the unsafe region) while predictions from both methods were shown with different symbols. For an error of 3% in the estimated failure probability a number of about 7 misplaced points should exist while in the case studied there are only 4 such points.

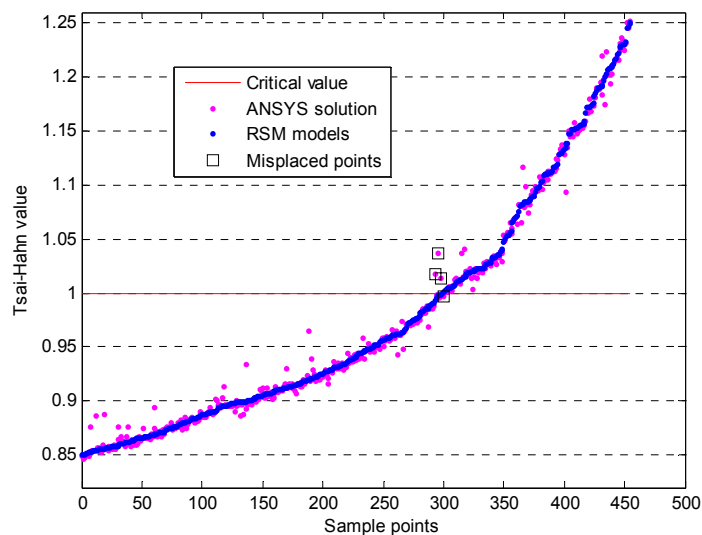


**Figure 20: Validation of the RSM predictions with Monte Carlo FE simulation results**

Similar satisfactory results with those shown in Figure 20 were also obtained for other layers and elements in the rotor blade including the element with the maximum probability of failure.

### 6.3 RSM and EDW assessment using THIN

The rotor blade was designed for extreme loading following the latest edition of IEC 61400-1. The material properties used were those shown in Table 6. The design values of the stress resultants as defined are shown for example in Table 7 for an inboard section. The element numbering of the section and the conventions of the direction of the stress resultants are shown in Figure 21.

**Table 6: Material properties**

| Property       | Mean Value | St. Deviation | $R_d$ |
|----------------|------------|---------------|-------|
| $E_1$ (GPa)    | 22.9       | 2.1           | 22.9  |
| $E_2$ (GPa)    | 7.9        | 1.6           | 7.9   |
| $\nu_{12}$     | 0.3        | 0.05          | 0.3   |
| $G_{12}$ (GPa) | 1.7        | 0.4           | 1.7   |
| $X_T$ (MPa)    | 241.2      | 34.4          | 134.2 |
| $X_C$ (MPa)    | 199.5      | 19.9          | 123.6 |
| $Y_T$ (MPa)    | 22.0       | 3.6           | 11.5  |
| $Y_C$ (MPa)    | 89.3       | 9.1           | 55.1  |
| S (MPa)        | 9.7        | 1.4           | 5.4   |

**Table 7: Design and stochastic load parameter values**

| Stress Resultant | $F_d$   | Gumbel parameter a | Gumbel parameter b |
|------------------|---------|--------------------|--------------------|
| $N_x$ (kN)       | 306.00  | 1.297              | 243.6              |
| $N_y$ (kN)       | 200.50  | 5.163              | 155.6              |
| $N_z$ (kN)       | 145.87  | 4.289              | 112.7              |
| $M_x$ (kNm)      | 17.80   | 0.667              | 13.6               |
| $M_z$ (kNm)      | 1872.50 | 50.610             | 1451.3             |
| $M_y$ (kNm)      | 1253.75 | 35.510             | 970.4              |

The maximum R-factor values of each element for the section used as an example are presented in Figure 22, right ordinate axis. Failure is indicated when  $R < 1$ . The abscissa in these graphs stand for the element number, see Figure 21. There is a significant number of elements that fail according to IEC for the section studied here as an example. Failure of these elements is due to matrix cracks at the off-axis plies [90], [+45], [-45]. This was revealed by implementing also the maximum stress failure criterion. Especially for the pressure side, failure concerns the [90] plies.

Reliability analysis using EDW, MC and RSM/MC was performed taking into account the stochastic nature of the material properties and the stress resultants. For the application with MC and RSM/MC also the correlation between the stress resultants was taken into account. Correlation matrix used is shown in Table 8. Probability of failure was estimated for every layer of every element and the maximum failure probability of each element is plotted in Figure 22 (left ordinate axis) for all probabilistic methods applied.

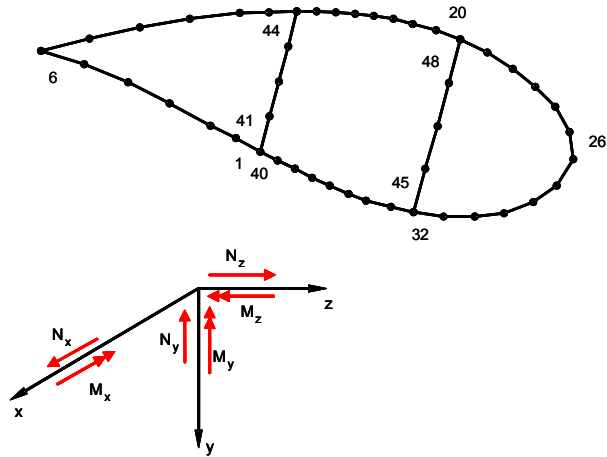


Figure 21: THIN section and extreme stress resultant direction

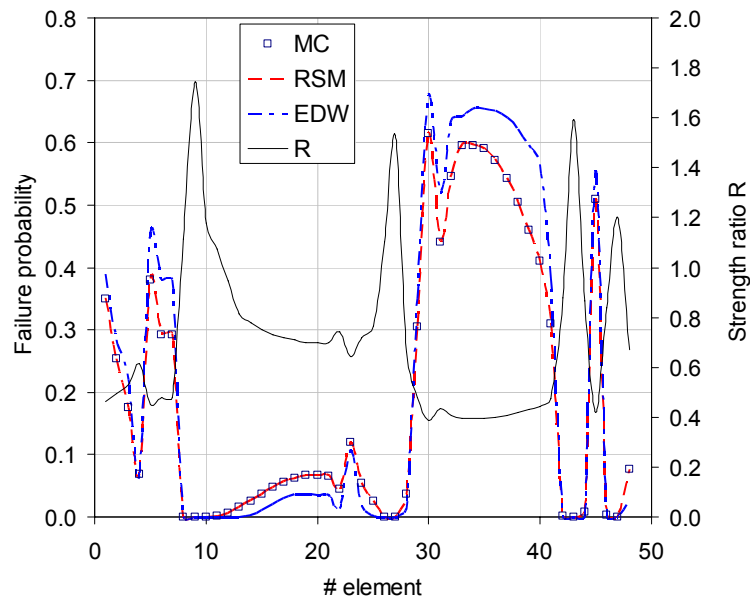


Figure 22: R-factor and Probability of failure,  $P_f$

Table 8: Correlation matrix for the stress resultants of the blade section

|                | N<br>(Axial) | $M_x$<br>(Torque) | $M_z$<br>(Flap) | $Q_y$<br>(Flap) | $M_y$<br>(Edge) | $Q_z$<br>(Edge) |
|----------------|--------------|-------------------|-----------------|-----------------|-----------------|-----------------|
| N (Axial)      | 1.00         | 0.00              | 0.00            | 0.00            | 0.00            | 0.00            |
| $M_x$ (Torque) | 0.00         | 1.00              | 0.48            | 0.53            | 0.77            | 0.79            |
| $M_z$ (Flap)   | 0.00         | 0.48              | 1.00            | 0.95            | 0.33            | 0.32            |
| $Q_y$ (Flap)   | 0.00         | 0.53              | 0.95            | 1.00            | 0.28            | 0.27            |
| $M_y$ (Edge)   | 0.00         | 0.77              | 0.33            | 0.28            | 1.00            | 0.99            |
| $Q_z$ (Edge)   | 0.00         | 0.79              | 0.32            | 0.27            | 0.99            | 1.00            |

High values of failure probabilities are developed for the section studied. These are the consequences of matrix cracks developed in the off-axis plies.

Both deterministic as well as probabilistic results reveal that the critical parts (with respect to the specific damage mode of matrix cracks) for the section are especially located at the pressure side of the blade.

A comparison between RSM/MC and EDW with direct MC reveals that RSM predictions are highly accurate even at very low probabilities. This is not the case of EDW which follows the trend, yet lacks in accuracy. However, this result might be the effect of not taking into account the correlation of the stress resultants in the EDW. Finally, it must be noticed that the time needed for the direct MC simulations are 13 hours (for the root section) while 3 hours are needed for RSM/MC and 10 sec for EDW in an ordinary PC.

## 7. Conclusions

A computational procedure was developed that may be easily combined with currently available aero-elastic codes, for the probabilistic assessment of wind turbine rotor blades. This was achieved by combining the methodologies developed for the probabilistic assessment of laminates under general in-plane loading and that developed for the automatic, deterministic strength analysis of rotor blades, in an integrated software tool. The stochastic characterization of composite material properties was implemented at the ply level where the reliability analysis was also performed. This is in agreement with guidelines of wind turbine certification standards.

Implemented in the tool for the determination of structural reliability are two different probabilistic methods: Response Surface Method combined with Monte Carlo and Edgeworth expansion method. For the verification of the reliability estimations results were compared with simulation results of the Monte Carlo method and they were found in good agreement.

The purpose of the developed tool is to facilitate the incorporation of material property variability along with the load uncertainty in an integrated structural design of a rotor blade. The software developed based on the Edgeworth expansion technique, through which a direct estimation of the reliability level of the rotor structure can be achieved, has a computational cost a little higher than any pure deterministic analysis tool. Thus, making it possible to be used during the design phase of the rotor blade, where a large number of loops should be performed before reaching the final structure. Results of the RSM/MC methodology implemented when compared to those by direct Monte Carlo simulation prove the degree of accuracy of the probabilistic method. The computational cost of the RSM/MC method is a bit higher computational cost than that of the EDW, still, much less than the cost of the crude Monte Carlo simulation. Therefore, it is anticipated that combination of these probabilistic methods as implemented in THIN analysis code could be used effectively in the future as a design tool for wind turbine blades, especially since the tool enables direct link with aeroelastic computational tools used for wind turbine simulations.

THIN is in fact a sectional analysis tool, providing aeroelastic codes input from the 3D composite rotor blade structure. It can also accept section stress resultants and perform detailed ply-by-ply stress/strain analyses. The more sophisticated the beam theory implemented in the finite element structural module of the aeroelastic code, the more accurate the results for the stress field to be derived. Nonetheless, the potential offered from such an analysis is indisputable. First of all, it is the first time that the variation of the elasticity properties of the blade (sections) are estimated and could be potentially incorporated in an aero-elastic analysis including both variability of the loading (wind induced) and the structure, resulting in the estimation of the interaction between the environment and the structure in statistical terms. Secondly, structural modifications of the blade, even on the layer level (e.g. addition or removal of a layer in the blade), can be easily adopted and be accounted for in the aero-elastic analysis without having the need to pass through a more costly three-dimensional finite element model.

Additionally, the immediate reliability estimation on the layer level makes possible the optimization of the structure even during the initial phases of the design, therefore reducing the necessary design loops up to the final design. It should be mentioned that code THIN was initially used in fatigue calculations of the blade in [26]; therefore, it would be possible to extend the current probabilistic approach towards an integrated probabilistic design including fatigue.

On the other hand within the present work the advantages and limitations of the developed methodology for the estimation of the failure probability under extreme loads using 3-D shell finite element model of the wind turbine blade were extensively discussed. The work conducted on the RSM methodology, showed that use of 3D finite element models, with an accurate representation of the structure, using load data as delivered by aero-elastic computational tools for wind turbines involves a number of assumptions, introducing uncertainties in the final model estimations.

## 8. References

- [1]. Braam H, Christensen CJ, Ronold KO, Thogersen ML. PRODETO, a computer code for probabilistic fatigue design. Proc. of EWEC 1999: "Wind Energy for the next Millenium", Nice, France, 1-5 March 1999, eds. E.L. Petersen, P. Hjulær Jensen, K. Rave, P. Helm, H. Ehmann, publ. James & James Science Publishers, London, 1999
- [2]. Veldkamp D. Chances in Wind Energy: A probabilistic approach to wind turbine fatigue design. PhD Thesis, DUWIND Delft University Wind Energy Research Institute, 2006
- [3]. Ronold KO, Larsen GC. Reliability-based design of wind-turbine rotor blades against failure in ultimate loading, *Engineering Structures* 2000; 22: 565-574
- [4]. Madsen HO, Krenk S, Lind NC. *Methods of structural safety*, Prentice-Hall, Inc.: New Jersey, 1986
- [5]. Ditlevsen O, Madsen HO. *Structural reliability methods*, John Wiley and Sons, 1996
- [6]. Tvedt L. Proban – probabilistic analysis. *Structural Safety* 2006; 28(1-2): 150-163
- [7]. Gollwitzer S, Kirchgaessner B, Fischer R, Rackwitz R. PERMAS-RA/STRUREL system of programs for probabilistic reliability analysis. *Structural Safety* 2006; 28(1-2): 108-129
- [8]. Winterstein SR, Veers PS. Theory manual for FAROW Version 1.1: A numerical analysis of the fatigue and reliability of wind turbine components, SAND94-2459, 2000
- [9]. Janssen LGJ, van Wingerde AM, Mishnaevsky LJr, Philippidis TP. Detailed Plan of Action, WP3: Rotor Structures and Materials. UPWIND Technical Report, [www.upwind.eu](http://www.upwind.eu), 2006
- [10]. Tsai SW, Hahn HT. *Introduction to composite materials*. Technomic Publishing Co.: Westport, 1980
- [11]. IEC 61400-1:2005 "Wind Turbines - Part 1: Design Requirements", 3rd Edition, 2005
- [12]. Germanischer Lloyd Industrial Services GmbH, Rules and Guidelines, IV Industrial Services, Part 1 Guideline for the Certification of Wind Turbines, 2010
- [13]. DNV-OS-J102, Design and Manufacture of Wind Turbine Blades, Offshore and Onshore Wind Turbines, 2006, with amendments 2007
- [14]. Veers PS, Ashwill TD, Sutherland HJ, Laird DL, Lobitz DW, Griffin DA, Mandell JF, Musial WD, Jackson K, Zuteck M, Miravete A, Tsai SW, Richmond JL. Trends in the design, manufacture and evaluation of wind turbine blades. *Wind Energy* 2003; 6: 245-259
- [15]. Philippidis TP, Roupakias GS, Vionis P. Assessment of composite rotor blade structural modelling efficiency through comparison of FEM numerical results and experimental data. Proc. of EWEC 94, pp. 155-160, ed. JL. Tsipouridis, 1994

- [16]. Kong C, Bang J, Sugiyama Y. Structural investigation of composite wind turbine blade considering various load cases and fatigue life. *Energy* 2005; 30: 2101-2114
- [17]. Philippidis TP, Kyrsanidi N, Passipoularidis VA, Antoniou A, 30m split-blade design, Deliverable WP5 within the Energie project #ENK5-CT2000-00328: Development of a MW scale wind turbine for high wind complex terrain sites (MEGAwind), University of Patras, 2002
- [18]. IEC 61400-1:1999, Wind Turbine Generator Systems- Part 1: Safety requirements, 2nd edition
- [19]. Bacharoudis KC, Philippidis TP, Structural reliability analysis of a composite rotor blade in ultimate loading, in Proc. of the EAWE 3rd Conference: "The Science of making Torque from Wind" TORQUE 2010, Ed. S. Voutsinas, T. Chaviaropoulos, pp. 811-828, Heraklion, Crete, Greece, 2010
- [20]. Malcolm DJ, Laird DL. Modeling of blades as equivalent beams for aeroelastic analysis. AIAA-2003-870; 41st Aerospace Sciences Meeting and Exhibit, Reno, Nevada, Jan. 6-9, 2003
- [21]. Riziotis VA, Voutsinas SG, Politis ES, Chaviaropoulos PK. Aeroelastic Stability of Wind Turbines: The Problem, the Methods, the Issues. *Wind Energy* 2004; 7: 373-392
- [22]. Jonkman JM, Buhl ML Jr. Fast User's Guide. NREL Technical Report, NREL/EL-500-38230, 2005
- [23]. Lekou DJ, Philippidis TP, PRE-and POST\_THIN: A Tool for the Probabilistic Design and Analysis of Composite Rotor Blade Strength. *Wind Energy* 2009; 12(7):676-691
- [24]. Malcolm DJ, Laird DL. Extraction of Equivalent Beam properties from blade models. *Wind Energy* 2007; 10: 135-157
- [25]. Hodges DH, Yu W. A rigorous, engineer-friendly approach for modelling realistic, composite rotor blades. *Wind Energy* 2007; 10: 179-193
- [26]. Philippidis TP, Vassilopoulos AP, Katopis KG, Voutsinas SG. THIN/PROBEAM: A software for fatigue design and analysis of composite rotor blades. *Wind Engineering* 1996; 20(5): 349-362
- [27]. Lekou DJ, Philippidis TP. Mechanical Property variability and its Effect on Failure Prediction. *Composites Part B: Engineering* 2008; 39: 1247-1256
- [28]. Lekou DJ, Philippidis TP. Influence of mechanical property variability on failure prediction of FRP laminates. Proc. of the 27th Risø International Symposium on Materials Science; Polymer Composite Materials for Wind Power Turbines, Roskilde, Denmark, Eds. H. Lilholt, B. Madsen, T. L. Andersen, L. P. Mikkelsen, A. Thygesen, 2006; 197-204
- [29]. Philippidis TP, Lekou DJ, Baharoudis C. Assessment of failure probability under uni-axial and multi-axial static and fatigue load. OPTIMAT BLADES report, OB\_TG2\_R035\_rev.000, [www.wmc.eu/public\\_docs/index.htm](http://www.wmc.eu/public_docs/index.htm), 2006
- [30]. Philippidis TP, Eliopoulos EN, Bacharoudis K, Masmanidis I, Assimakopoulou TT, Test Results of In-Plane Mechanical Properties for Modeling Complex Stress States, UPWIND Deliverable D.3.3.6, University of Patras, 2010
- [31]. Fitzwater LM, Winterstein SR, Predicting design wind turbine loads from limited data: Comparing random process and random peak models, *J. Solar Energy Eng.* 2001; 123(4):364-372
- [32]. Veers PS, Butterfield S, Extreme load estimation for wind turbines: Issues and opportunities for improved practice, En 2001 ASME Wind Energy Symposium, AIAA/ASME, 2001
- [33]. Peeringa JM. Extrapolation of extreme responses of a multi megawatt wind turbine. ECN Report, ECN-C--03-131, 2003

- [34].Moriarty PJ, Holley WE, Butterfield SP, Extrapolation of extreme and fatigue loads using probabilistic methods, Technical report NREL/TP-500-34421, National Renewable Energy Laboratory NREL, Golden, Colorado, USA, September 2003
- [35].Genz R, Nielsen KB, Madsen PH, An investigation of load extrapolation according to IEC 61400-1 Ed.3. EWEC 2006
- [36].Cheng PW, Bierbooms WAAM, Distribution of extreme gust loads of wind turbines, Journal of Wind Engineering and industrial Aerodynamics 2001; 89: 309-324.
- [37].Bacharoudis KC, Lekou DJ, Philippidis TP, Structural reliability analysis of rotor blades in ultimate loading, Submitted for publication, 2011
- [38].IEC/TS 61400-23:2001, Wind turbine generator systems – Part 23: Full-scale structural testing of rotor blades, 1<sup>st</sup> edition
- [39].Hinton MJ, Soden PD. Failure criteria for composite laminates. Comp. Sci. and Techn. 1998; 58: 1001-1010
- [40].Soden PD, Hinton MJ, Kaddour AS. Comparison of the predictive capabilities of current failure theories for composite laminates. Comp. Sci. and Techn. 1998; 58: 1225-1254
- [41].Hinton MJ, Kaddour AS, Soden PD. Comparison of the predictive capabilities of current failure theories for composite laminates judged against experimental evidence. Comp. Sci. and Techn. 2002; 62: 1725-1797
- [42].Puck A, Festigkeitsberechnung an Glasfaser/Kunststoff - Laminaten bei zusammengesetzter Beanspruchung; Bruchhypothesen und Schichtenweise Bruchanalyse, Kunststoffe, Bd. 59, Heft 11, pp.780-787, 1969
- [43].Puck A, Festigkeitsanalyse von Faser-Matrix-Laminaten; Modelle für die Praxis, Carl Hanser Verlag, 1996
- [44].Lekou DJ, Philippidis TP, Probabilistic Strength Assessment of FRP Laminates; Verification and comparison of analytical models, UPWIND Deliverable Report D.3.3.2, 2007
- [45].Tsai SW. Theory of composite design. Think Composites, 1992
- [46].Jones RM. Mechanics of composite materials. McGraw-Hill, 1975
- [47].Ang AH-S, Tang WH. Probability concepts in engineering planning and design, Vol. II: Decision, risk and reliability, John Wiley & Sons, 1984
- [48].Pellisetti MF, Schueller GI. On general purpose software in structural reliability – An overview. Structural Safety 2006; 28(1-2): 3-16
- [49].Miki M, Murutsu Y, Tanaka T, Shao S. Reliability of unidirectional fibrous composites. AIAA Journal 1990; 28(11): 1980-1986
- [50].Wetherhold RC, Ucci AM. Probability techniques for reliability analysis of composite materials, NASA CR-195294, 1994
- [51].Myers RH, Montgomery DC, Response Surface Methodology: Process and Product Optimization Using Designed Experiments, John Wiley, New York, 2002
- [52].Simpson TW, Peplinski JD, Koch PN, Allen JK, On the use of statistics in design and the implications for deterministic computer experiments, Proc. of DET'97, 1997 ASME Design Engineering Technical Conferences, September 14-17, Sacramento, California, 1997
- [53].Bucher CG, A Fast and efficient response surface approach for structural reliability problems, Structural safety 7: 57-66, 1990
- [54].Rajashekar MR, Ellingwood BR, A new look at the response surface approach for reliability analysis, Structural safety 1993; 12: 205-220
- [55].Wetherhold RC. Reliability calculations for strength of a fibrous composite under multiaxial loading. J. of Comp. Mater. 1981; 15: 240-248

- [56]. Philippidis TP, Lekou DJ. Probabilistic failure prediction for FRP composites. *Comp. Scie. and Techn.* 1998; 58: 1973-1982
- [57]. Philippidis TP, Lekou DJ. A probabilistic approach to failure Prediction of FRP laminated composites. *Mech. of Comp. Mater. & Struct.* 1998; 5: 371-382
- [58]. Cramer H. *Mathematical methods of statistics.* Princeton University Press, 1971
- [59]. Bjerager P. Methods for structural reliability computations. In: *Reliability Problems; General Principles and applications in mechanics of solids and structures.* Eds. F. Casciati, J. B. Roberts, Publ. Springer Verlag, 1991; 89-135
- [60]. Nowak AS, Collin KR. *Reliability of structures.* McGraw-Hill, 2000
- [61]. Knuth DE. *The art of computer programming, Vol. 2: Seminumerical algorithms.* Addison Wesley Longman, 1998
- [62]. DIAB International AB. Divinycell HP, Technical Manual, [www.diabgroup.com](http://www.diabgroup.com), 2007